REPORT NO.
UCSESM 71-4

STRUCTURES AND MATERIALS RESEARCH
DEPARTMENT OF CIVIL ENGINEERING

A COMPUTER PROGRAM FOR ANALYSIS OF STIFFENED PLATES UNDER COMBINED INPLANE AND LATERAL LOADS

by
DAG KAVLIE
RAY W. CLOUGH

This research was sponsored by the Structures Department of the Naval Ship Research and Development Center under Naval Ship Systems Command Subproject SF 013 0301, Task 1968, Contract N00014-69-A-0200-1045, continuation of Contract N00014-67-A-0114-0020.

MARCH 1971

STRUCTURAL ENGINEERING LABORATORY
UNIVERSITY OF CALIFORNIA
BERKELEY CALIFORNIA

Structures and Materials Research
Department of Civil Engineering

Report No. UCSESM 71-4

A COMPUTER PROGRAM FOR ANALYSIS OF STIFFENED PLATES UNDER COMBINED INPLANE AND LATERAL LOADS

by

Dag Kavlie

and

Ray W. Clough

This research was sponsored by the Structures Department of the Naval Ship Research and Development Center under Naval Ship Systems Command Subproject SF 013 0301, Task 1968, Contract N00014-69-A-0200-1045, continuation of Contract N00014-67-A-0114-0020.

Structural Engineering Laboratory
University of California
Berkeley, California

March 1971

ABSTRACT

The finite element method is used as the basis of a computer program for analysis of stiffened plates. Triangular and quadrilateral plate elements and beam elements may be used for idealization of the stiffened plates. The plate elements may have isotropic or orthotropic material properties. The stiffeners are assumed to be symmetric about the midplane of the plate. This assumption uncouples the plane stress and the plate bending problems. If the inplane stresses are not known in advance, the plane stress problem can be solved as a first step. The next step may be to solve the plate bending problem. The effect of the membrane stresses on the plate bending behavior is taken care of in this case by adding the geometric stiffness matrix to the elastic stiffness matrix. Alternatively the stability problem may be solved, finding the critical buckling eigenvalue and the corresponding mode shape. A listing of the FORTRAN IV computer program is given in the report, and a few examples of bending and buckling of stiffened plates are presented. The program has been developed and tested on the CDC 6400 computer.

ACKNOWLEDGEMENT

This research was sponsored by the Department of Structural Mechanics, Naval Ship Research and Development Center under the Naval Ship Systems Command Subproject SF 013 0301, Task 1968, Contract N00014-67-A-0114-0020.

A major part of the element stiffness subroutines was developed and programmed by Dr. Carlos Felippa. Soheil Mojtahedi carried out most of the testing of the computer program on the numerical examples described in Section IV.

TABLE OF CONTENTS

I. INTRODUCTION

The analysis of stiffened plates subjected to inplane and lateral loads plays an important role in the design of ship structures. A commonly used approach in the past has been based on the grillage idealization where the stiffened plate is represented by a system of intersecting beams [1]. For plate fields having many stiffeners, orthotropic plate theory usually has been applied [2, 3]. Within the last 15 years the more general finite element technique has been developed for analysis of plates and shells of arbitrary geometry [4, 5, 6]. One of the most important advantages of the finite element technique is that an assembly of different structural elements such as plates and beams can be dealt with in a single coordinated analysis. The finite element program described in this report can include quadrilateral and triangular plate elements, and also beam type elements. However, eccentricity of the stiffeners is not included because a different idealization for the stiffeners would have to be used to account for that effect. The simplified idealization used here makes it possible to uncouple the membrane analysis from the bending analysis. The effect of membrane forces on the plate bending behavior can, however, be taken into account by adding the geometric stiffness terms to the bending stiffness of plates and stiffeners.

If the effect of stretching of the midplane of the plate as a result of lateral displacement were to be included, an iterative analysis procedure would have to be used. This would correspond to a second order theory of plates, and is not included in the present version of the program. An extension of the present program to include this effect would be possible with a moderate effort. The linearized theory

presented here is expected to give satisfactory accuracy for displacements less than half the plate thickness. This means that a large number of problems of practical importance can be solved by means of the computer program described.

II. METHOD OF ANALYSIS

1. Discretization

The stiffened plate is idealized as an assemblage of flat plate elements symmetric about the mid-plane of the plate. For a plate with eccentric stiffening, the fact that the plate will act as a flange for the stiffeners can be taken into account only in an approximate way. To carry out such an analysis, an effective width of plate flange must be used when computing the moment of inertia of the stiffeners. In the membrane analysis the stiffeners are idealized as bar elements taking axial forces. In the bending analysis the stiffeners are idealized as beam elements. For plates with many stiffeners with equal spacing, the stiffened plate field may be idealized as an orthotropic plate. The quadrilateral and triangular elements used in this program permit orthotropic material properties to be represented.

2. Coordinate System and Sign Conventions

The plate is referred to a global right handed cartesian system x-y-z, with x-y in the undeformed midsurface. Positive sign conventions for displacements and rotations of the midsurface joints are indicated in Fig. 1.

Concentrated transverse forces P and concentrated moments C_x, C_y follow the sign convention of transverse displacements w and rotations θ_x, θ_y, respectively. A lateral distributed load q (x, y) is also positive in the direction of a positive displacement w (upwards). For the internal moments the sign convention is indicated in Fig. 2. Note that this implies that a positive normal moment produces compression in the upper surface of the plate (deforms the plate into convex downward curvature).

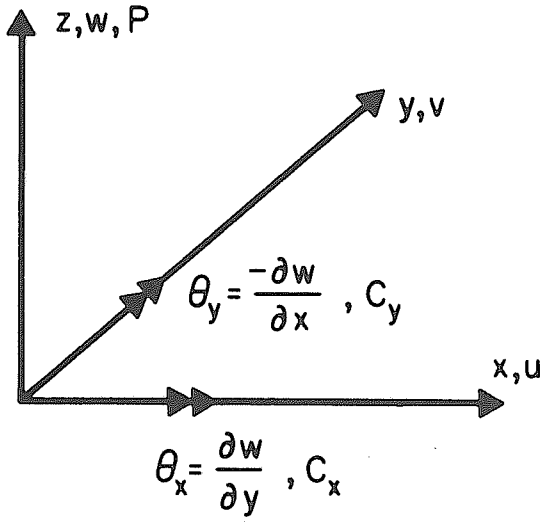

FIG. 1 DISPLACEMENT AND FORCE SIGN CONVENTION

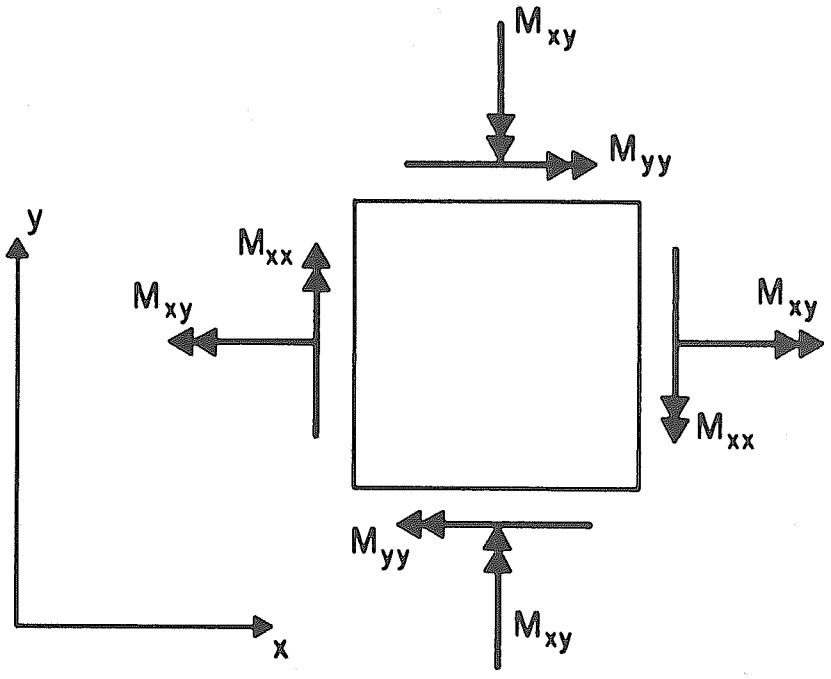

FIG. 2 SIGN CONVENTION FOR x-y MOMENTS

3. Finite Elements Used

The finite elements used in the two major steps of the analysis will be described briefly in this section:

i) Plane Stress Analysis

The elements used for this part of the analysis all have two degrees of freedom for each nodal point, u- and v- displacements. The set of elements includes: Bar element (BAR) with 2 nodal points, Constant Strain Triangular element (CST) with 3 nodal points and Quadrilateral Plane Stress element with 4 external nodal points (QUPS-10). The latter element also has one internal point. This is eliminated by static condensation, so the final element stiffness matrix is a 8 x 8 matrix. Derivation of the stiffness matrices is described in [6] for the quadrilateral and triangular elements and in [8] for the bar element. Note that the element stiffness matrices are formed directly in the global coordinate system so that no transformations from local to global coordinates are required. Fig. 3 shows the membrane elements used. The derivation of the stiffness matrix for the BAR and the CST elements is performed analytically, while for the QUPS-10 element a numerical integration is carried out using a 4th order Gaussian integration formula (16 interior integration points).

ii) Plate Bending Analysis

The elements used for plate bending all have three degrees of freedom for each nodal point, w transverse displacement (normal to the midplane of the plate) and θ_x and θ_y rotations about the x- and y-axes. The beam element used accounts for shear as well as flexural deflection [8]. The basic assumption in the program is that stiffeners are symmetric about the midplane of the plate. A stiffener which is

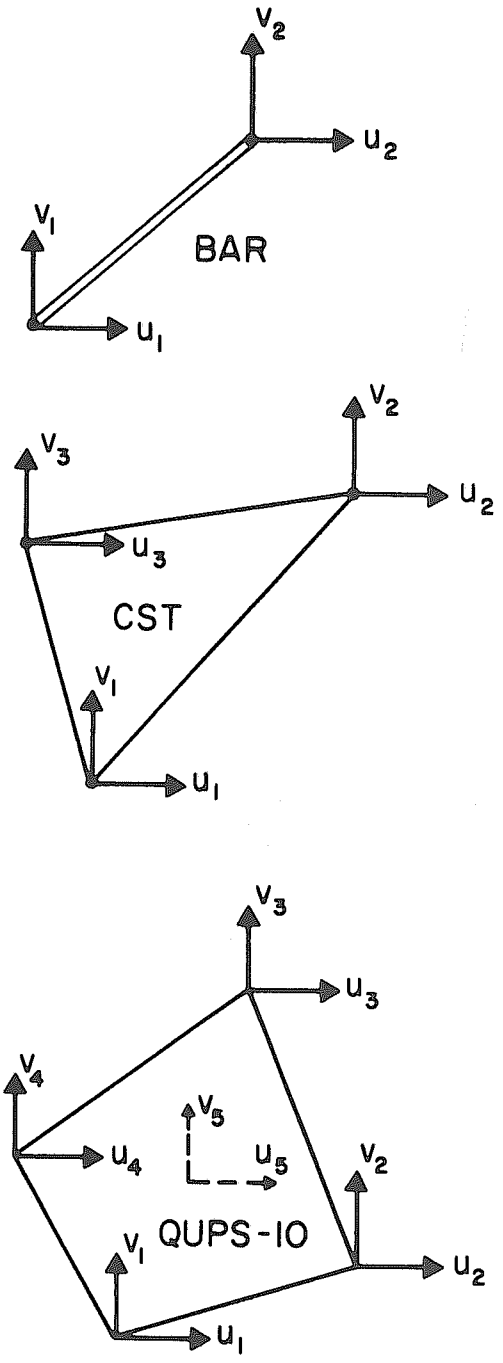

FIG. 3 PLANE STRESS ELEMENTS

not symmetric about the midplane should have an effective width of plating included when the moment of inertia is computed [9]. If a more refined finite element representation had been used, this approximation would not have been necessary, but it then would have been necessary to solve a 3-dimensional problem including both bending and plane stress stiffnesses in the same analysis.

The triangular plate bending element LCCT-9 is derived in [5]. This element is fully compatible and has a linearly varying slope along the external sides. A triangular element with a parabolic slope variation and 12 degrees of freedom (LCCT-12) is derived in the same reference. The quadrilateral plate bending element Q-19 is assembled of four triangular elements which have parabolic and linear slope variations along the interior and external sides, respectively (see Fig. 4). The seven internal degrees of freedom are eliminated from these elements by static condensation. The final quadrilateral plate bending element has 12 external degrees of freedom and a 12 x 12 element stiffness matrix. This element is described in detail in [7].

4. Geometric Stiffness

If a plate field is subjected to a system of combined inplane and lateral loads, the linear theory is no longer valid and there exists a coupling between the membrane and the plate bending actions. This problem is covered by the second order theory of plates, the Von Karman theory. If one neglects the influence of lateral displacements on the membrane strains, however, one is still able to solve the membrane and plate bending problems separately. The effect of membrane stress resultants N_x, N_y and N_{xy} on the plate bending problem, can be dealt with by adding the "geometric stiffness" or "initial stress" matrix to

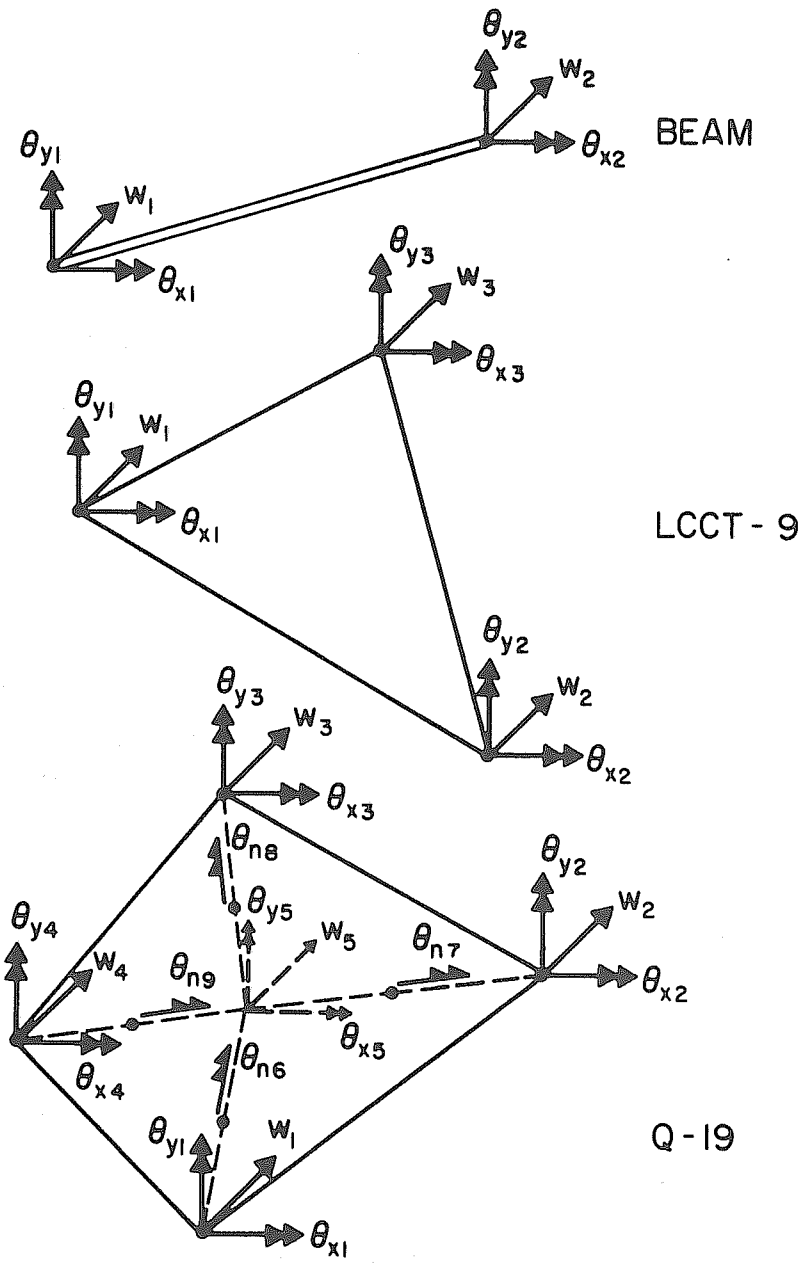

FIG. 4 PLATE BENDING ELEMENTS

elastic plate bending stiffness matrix. Lateral displacements and moments are still linear with respect to lateral loads, but nonlinear with respect to inplane loads. This corresponds to the beam-column theory of beams.

The work of the inplane stress resultants due to the mid-plane rotations $w_{,x}$ and $w_{,y}$ is given by the following expression:

$$U_G = \frac{1}{2} \int_A [N_x(w_{,x})^2 + N_y(w_{,y})^2 + 2N_{xy}(w_{,x})(w_{,y})] \, dA \qquad (1)$$

Fig. 5 gives a geometrical illustration of the work done by the N_x stress resultant. In matrix form Eq. 1 can be written as:

$$U_G = \frac{1}{2} \int < w_{,x} \quad w_{,y} > \begin{bmatrix} N_x & N_{xy} \\ N_{xy} & N_y \end{bmatrix} \begin{Bmatrix} w_{,x} \\ w_{,y} \end{Bmatrix} dA \qquad (2)$$

For a plate bending element the displacement w is defined, by interpolation functions $< \phi_w >$, in terms of the nodal point displacements $\{r\}$, as follows:

$$w = < \phi_w > \{r\} \qquad (3)$$

Differentiating the expansion for w with respect to x and y yields:

$$\begin{aligned} w_{,x} &= < \phi_{w_{,x}} > \{r\} \\ w_{,y} &= < \phi_{w_{,y}} > \{r\} \end{aligned} \qquad (4)$$

and substituting these into the expression for U_G leads to:

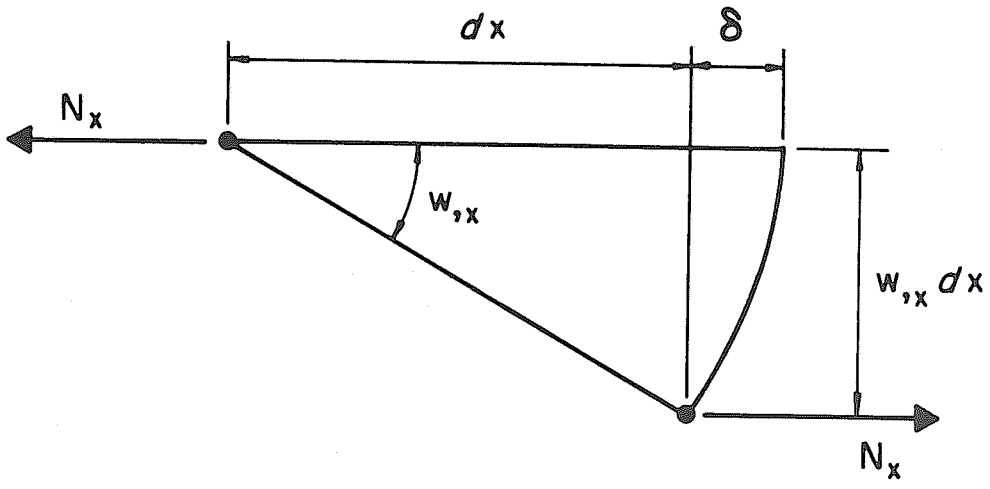

$$\delta = \left(\sqrt{1+w_{,x}^2}-1\right)dx \approx (w_{,x})^2 dx/2$$

$$dU_{Gx} = N_x (w_{,x})^2 dA/2$$

FIG. 5 ILLUSTRATION OF THE WORK DONE BY N_x STRESS RESULTANT DUE TO $w_{,x}$ ROTATION

$$U_G = \frac{1}{2} \{r\}^T [k_G] \{r\} \tag{5}$$

where $[k_G]$ is the element geometric stiffness and is expressed by:

$$[k_G] = \int_A \left[\phi_{w,x}^T \vdots \phi_{w,y}^T \right] \begin{bmatrix} N_x & N_{xy} \\ N_{xy} & N_y \end{bmatrix} \begin{bmatrix} \phi_{w,x} \\ \hline \phi_{w,y} \end{bmatrix} dA \tag{6}$$

The total potential energy of the element can be written as

$$\pi = U + U_G - w_E \tag{7}$$

where $U = \frac{1}{2} \{r\}^T [k_c] \{r\}$ and $w_E = \{r\}^T \{R\}$; $[k_c]$ and $\{R\}$

representing the elastic stiffness matrix and nodal load vector of the element, respectively. Taking the variation of the potential energy with respect to the nodal displacements, and setting the result equal to zero, $\delta\pi = 0$, leads to:

$$[\underline{k}_c - \underline{k}_G] \{r\} = \{R\} \tag{8}$$

As can be seen, for each plate bending element, the geometric stiffness matrix $\underline{k}_G$ is directly added to the elastic stiffness matrix $\underline{k}_c$ to obtain the total stiffness matrix. The elastic and geometric stiffness matrices $\underline{K}_c$ and $\underline{K}_G$ of the complete structure are then obtained by assembling those of the individual elements. The equilibrium equation of the structure then can be written as:

$$[\underline{K}_c - \underline{K}_G] \{\overline{r}\} = \{\overline{R}\} \tag{9}$$

where $\{\overline{r}\}$ and $\{\overline{R}\}$ are nodal point displacement and load vectors of the complete structure, respectively.

A special case applies when no lateral loads are present, i.e., $\{\overline{R}\} = \{0\}$. Equation (9) now becomes the equation defining the stability of the plate. If all the inplane stress resultants are increased by a factor λ, the plate becomes unstable, and the corresponding values of the inplane forces represent the buckling load:

$$\begin{aligned} N_{xc} &= \lambda N_x \\ N_{yc} &= \lambda N_y \\ N_{xyc} &= \lambda N_{xy} \end{aligned} \tag{10}$$

The problem of finding this buckling load factor λ is a standard eigenvalue problem:

$$[K_c]\{\overline{r}\} = \lambda [K_G]\{\overline{r}\} \tag{11}$$

Note that in Eq. (11) compression is taken to be positive, to give a positive eigenvalue.

It should be noted that the interpolation functions $< \phi_w >$ employed in deriving the geometric stiffness do not have to be identical to those used for calculation of the elastic stiffness matrix. Clough and Felippa (7) have compared three different assumptions for $< \phi_w >$ in the derivation of the geometric stiffness for plate bending. The simplest is the linear assumption:

$$< \phi_{w1} > = < \zeta_1 \ \zeta_2 \ \zeta_3 > \tag{12}$$

where ζ_i are the triangular coordinates of the element, as described in Appendix A. Secondly, a single cubic expansion $< \phi_{w3} >$ and finally the compatible cubic expansion $< \phi_{wc} >$ used in the derivation of the elastic stiffness matrix in this study, were examined. Their conclusion was that the single cubic expansion $< \phi_{w3} >$ gave results almost identical to those obtained by the compatible cubic expansion and better than the linear expansion. The single cubic expansion is much simpler and therefore must be preferred for general analyses. In Appendix A the derivation of $\underline{k}_G$ for a triangular element using this expansion has been described in detail. For the derivation of geometric stiffness matrices for rectangular elements, the reader is referred to Gallagher and Gellatly [10] and Kapur and Hartz [15].

5. Arrangement of the Computer Program

The basic flowchart for the computer program is presented in Fig. 6. The subroutine SETUP inputs control parameters, geometric data, and material properties for the problem to be solved. For a quadrilateral plate field the quadrilateral elements may be generated in the computer program by specifying corner point coordinates and the number of elements to be used in each direction. Additional elements may be read in from cards. The option to read in all the nodal points and element data also exists, and the plate field may then have an arbitrary geometry. Depending on the parameter ND1, a plane stress analysis may be performed or the inplane stress state may be read in from cards. If a plate bending or buckling analysis is required, the next step will be to evaluate the plate bending elastic stiffness $\underline{k}_c$ and also the geometric stiffness $\underline{k}_G$ of the elements. If a plate bending analysis is required, the 19 x 19 stiffness matrix $\underline{k} = \underline{k}_c - \underline{k}_G$ is computed for each element

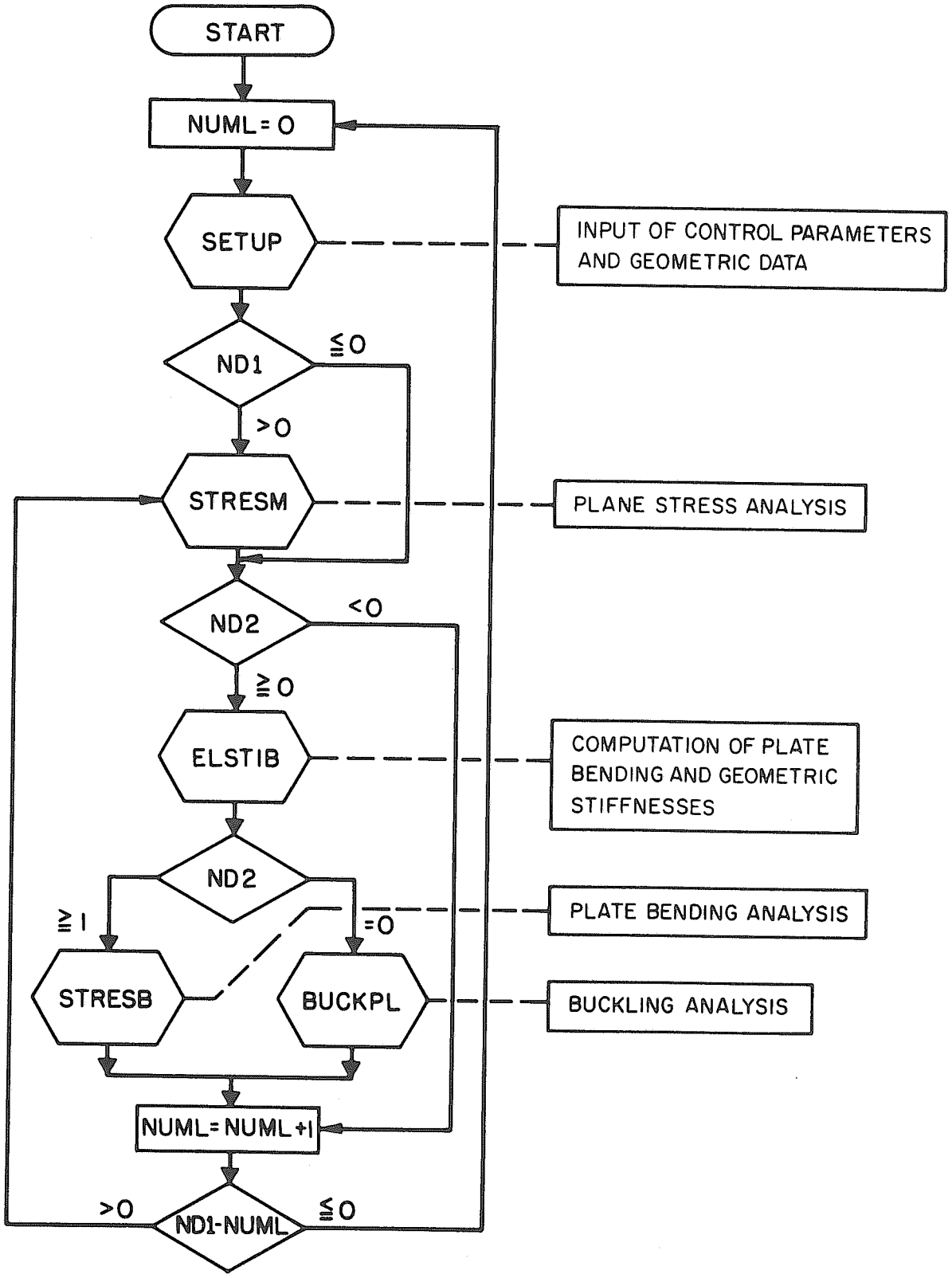

FIG.6 FLOW CHART FOR COMPUTER PROGRAM

and the 7 internal degrees of freedom are condensed. The resulting 12 x 12 stiffness matrix is written on tape. If a buckling analysis is to be performed, the full (19 x 19) element stiffnesses $\underline{k}_C$ and $\underline{k}_G$ for each element are written on tape for later use in the inverse iteration eigenvalue solution procedure.

The structure's stiffness matrix $\underline{K}$ is assembled by the direct stiffness method. Only the upper half band of the matrix is stored. The stiffness matrix is kept in the core memory. This restricts the capacity of the program to $b \times m < 18000$ for the 64K core memory on the CDC 6400, where b = half bandwidth of the stiffness matrix of the structure and m is the total number of degrees of freedom. For a bending problem this corresponds to NUMNP · (ND + 1) < 2000 where NUMNP is the total number of nodal points and ND is the maximum difference in nodal point numbers for a single element. The equilibrium equation may be written as:

$$\underline{K}\,\underline{r} = \underline{R} \tag{13}$$

where

$$\underline{K} = \underline{K}_C - \underline{K}_G \tag{14}$$

A Gaussian decomposition is performed on $\underline{K}$ for the solution of Eq. 13 as follows:

$$\underline{K} = \underline{L}\underline{D}\underline{L}^T \tag{15}$$

in which $\underline{L}$ is a lower triangular matrix. This is then used to solve Eq. 13 for the nodal displacements $\underline{r}$. Any specified number of load vectors may be included in $\underline{R}$

If the buckling stability of the system is to be evaluated, the eigenvalue problem obtained when $\underline{R} = 0$ must be solved; in this case the equation is written:

$$[K_c]\{u\} = \lambda [K_G]\{u\} . \tag{16}$$

Generally only the lowest eigenvalue is of interest, and it may be found conveniently by inverse interation. The efficiency of the process is improved in the present program by introducing a shift μ; i.e., the eigenvalue is represented by the sum of the shift and a reduced eigenvalue, δ:

$$\lambda = \mu + \delta. \tag{17}$$

Eq. 16 then becomes:

$$[\underline{K}_c - \mu \underline{K}_G]\{u\} = \delta [K_G]\{u\}, \tag{16a}$$

and the basic interation algorithm may be written

$$[\underline{K}_c - \mu \underline{K}_G]\{u^{(i+1)}\} = \delta [K_G]\{u^{(i)}\} = [K_G]\{v^{(i)}\}, \tag{18a}$$

where:

$$\{v\}^{(i+1)} = \delta \{u\}^{(i+1)} = \frac{\{u\}^{(i+1)}}{u_{max}^{(i+1)}} \tag{18b}$$

The initial assumed mode shape $\{v\}^{(o)}$ is found by computing the static displacements for a load condition which is read in. This displaced shape should include both symmetric and anti-symmetric components because the program may fail to determine a symmetric mode shape in case a completely anti-symmetric $\{v\}^{(o)}$ is supplied, or vice-versa. If no estimate for λ is available, the initial shift may be taken to be zero.

III - INPUT DATA INFORMATION

For any problem to be solved by the program, a group of punched cards will be required as follows:

1. START Card (A_6)

   The word "start" should be punched in columns 1 - 5.

2. Identification card (13 A 6)

   Alphanumeric information to be printed as a heading for the output should be punched in columns 1 - 78.

3. Control Cards

   The following two cards will be required:

   Card A - (5I4,F10.3)

Columns	1 - 4	NUMEL ($\leq$150)	Number of elements to be read in (generated elements excluded).
	5 - 8	NUMNP ($\leq$180)	Number of nodal points to be read in (generated nodal points excluded).
	9 - 12	NUMBC ($\leq$70)	Number of nodal points with boundary conditions to be read in (generated boundary conditions excluded).
	13 - 16	NMAT ($\leq$20)	Number of different materials (materials of beam and plate element are considered to be different in any problem).
	17 - 20	NUMPB ($\leq$50)	Number of points defining the boundary of the region where displacements and moments are to be plotted (mode shape in buckling analysis).

21 - 30	RT	Plate thickness for the quadrilateral field to be generated. (See "Element data cards").

Card B - (4L2, 3I2)

Columns 1 - 2	T1	Punch T if all quadrilateral elements are identical and have the same inplane stresses; otherwise punch F.
3 - 4	T2	Punch T if standard output without any intermediate data is needed; otherwise punch F.
5 - 6	T3	Punch T if all element and nodal point data is read in from cards; punch F if part of this data is to be generated (in the form of a quadrilateral mesh).
7 - 8	T4	Punch T if displacements and moments are to be plotted (mode shape in buckling analysis); punch F is no plot is needed.
9 - 10	ND1	Parameter which determines how inplane stress distribution should be obtained: = -2 Read in each nodal point value for σ_x, σ_y, τ_{xy}. = -1 Read in for each corner of the quadrilateral field the value of σ_x, σ_y, τ_{xy}. (This option must only be used when T3 = F). = 0 No inplane stress is present.

	≥1	Number of loading conditions for plane stress analysis
11 - 12	ND2	Parameter which determines type of lateral loading:
	< 0	No lateral load is present and a plane stress analysis only is to be performed
	= 0	Buckling analysis is to be performed.
	> 0	Number of loading conditions for plate bending analysis.
13 - 14	ND3	=1 if all quadrilateral elements are identical (regardless of inplane stress distribution).
		=0 otherwise.

4. Material Data Cards (I3, I2, 6 E 10.3)

For isotropic plate elements two constants, elastic modulus E and Poisson's ratio ν are read in. For orthotropic plate elements six constants, D_{11}, D_{22}, D_{33}, D_{12}, D_{13}, and D_{23} defining the 3 x 3 matrix in $\underline{\sigma} = \underline{D}\underline{\varepsilon}$ are read in. For beam elements, in addition to the elastic modulus E, the Poisson ratios ν_S and ν_T (used to define transverse and torsional shear moduli, $G_S = \frac{E}{2(1+\nu_S)}$ and $G_T = \frac{E}{2(1+\nu_T)}$ are read in.

For each material property one card (total of NMAT cards) is required:

Columns	1 - 3	Material number (*)
	4 - 5	Type of material constants:
		= 0 for isotropic plate elements.
		= 1 for orthotropic plate elements.
		= 2 for beam elements.

(*) For plate elements generated in the quadrilateral mesh this number should be set equal to 1.

6 - 15 E or D_{11}

16 - 20 ν, D_{22} or ν_s

21 - 30 ν_T or D_{33}

31 - 40 D_{12}

41 - 50 D_{13}

51 - 60 D_{23}

5. Boundary points defining plotting region (20 I4)

For plotting purposes a set of boundary points defining a plate contour must be punched in cyclic order (20 points per card). If no plot is needed leave a blank card.

6. Mesh generation cards

Two cards are required if a quadrilateral mesh is to be generated, i.e., T_3 = F:

Card A - ($2I_5$, 4(5X, 5I1))

Columns 1 - 5 NADIV Number of elements in ζ direction.

6 - 10 NBDIV Number of elements in η direction.

16 - 20 ICB Boundary conditions for side 1 (for u, v, w displacements and θ_x, θ_y rotations respectively, 0 = free, 1 = fixed)

26 - 30 Similarly for side 2

36 - 40 Similarly for side 3

46 - 50 Similarly for side 4

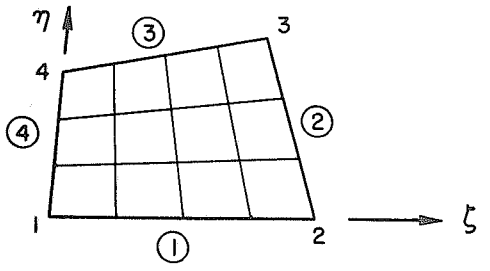

Numbering of corner points and sides of the generated quadrilateral mesh.

Card B - (8F 10.3)

Columns	1 - 10	XB (1)	x - coordinate of corner 1.
	11 - 20	XB (2)	x - coordinate of corner 2.
	21 - 30	XB (3)	x - coordinate of corner 3.
	31 - 40	XB (4)	x - coordinate of corner 4.
	41 - 50	YB (1)	y - coordinate of corner 1.
	51 - 60	YB (2)	y - coordinate of corner 2.
	61 - 70	YB (3)	y - coordinate of corner 3.
	71 - 80	YB (4)	y - coordinate of corner 4.

One should select the longer sides of the quadrilateral field as 1 - 2 and 3 - 4 in order to reduce the bandwidth of the stiffness matrix and also to obtain better plots.

7. Element Data Cards (6I4,6X,4F10.3)

If all the elements are generated, i.e., NUMEL = 0, no card is required.

Nodal points should be ordered counter-clockwise aroung the plate element. All elements of the structure are numbered in natural sequence. Generated elements are numbered first and numbering of the additional elements, if any, follows that of the generated ones. Each element card should have the following information:

Columns	1 - 4	Element number
	5 - 8	Nodal point I
	9 - 12	Nodal point J
	13 - 16	Nodal point K (repeat J for beam element)
	17 - 20	Nodal point L (repeat J for beam element, I for triangular element)
	21 - 24	Material number
	31 - 40	Plate thickness or cross-sectional area of the beam element (plate thickness will be set equal to

reference thickness if this space is left blank)

41 - 50 Moment of inertia of the beam element.

51 - 60 Torsional inertia of the beam element.

61 - 70 Shear area of the beam element. (If shear deflection is neglected this space should be left blank.)

In general one card for each additional element is required; however, if some element cards are omitted the program automatically generates the omitted information by incrementing I, J, K and L by one for each element. Material identification is set equal to that on the card previously read; so are all sectional properties of the element.

8. Nodal point cards (I4, 2F10.3)

If all the nodal points are generated, i.e., NUMNP = 0, no card is required.

Columns 1 - 4 Nodal point number

5 - 14 x - coordiante

15 - 24 y - coordinate

Nodal points must be numbered and read in natural sequence. Numbering of additional nodal points, if any, should follow that of the generated ones. If some nodal point cards are omitted, the corresponding points are generated at equal intervals along a straight line between defined nodal points.

9. Boundary condition cards (2I4, 2X, 5I1, 5X, 6F10.3)

If all the boundary conditions are generated, i.e., NUMBC =0, no card is required.

One card is required for each additional point at which boundary conditions are prescribed.

Columns 1 - 4 Boundary point number.

5 - 8	Nodal point number of the boundary point.
11 - 15	Boundary conditions for u, v, w displacements and θ_x, θ_y rotations, respectively (0 = free, 1 = fixed).
21 - 30	Prescribed constraint angle for the boundary point (measured counter-clockwise from the x - axis).
31 - 40	Given u displacement.
41 - 50	Given v displacement.
51 - 60	Given w displacement.
61 - 70	Given θ_x rotation.
71 - 80	Given θ_y rotation.

10. Input of inplane stresses

If NDl $\geq$ 0 no card is required, otherwise two groups of cards are required for reading the inplane stresses of the plate elements and the axial stresses of the beam elements:

Group A - Inplane stresses of the plate elements:

Depending on the value of NDl, one of the following two sets of cards is required:

Al: (NDl = -2), (I4, 3Fl0.3)

Inplane stress distribution is read in for each nodal point. One card for each nodal point is required:

Columns	1 - 4	Nodal point number.
	5 - 14	σ_x stress at the nodal point.
	15 - 24	σ_y stress at the nodal point.
	25 - 34	τ_{xy} stress at the nodal point.

A2:(NDl = -1), (4Fl0.3)

Inplane stress is read in for each corner point of the quadrilateral field. Three cards are required.

Columns 1 - 10 σ_x stress at the corner point 1 of the quadrilateral field.

11 - 20 σ_x stress at the corner point 2 of the quadrilateral field.

21 - 30 σ_x stress at the corner point 3 of the quadrilateral field.

31 - 40 σ_x stress at the corner point 4 of the quadrilateral field.

The same is repeated for σ_y and τ_{xy}.

Group B - Axial stresses in the beam elements:

The following cards are required:

B1: (I4)

Columns 1 - 4 Number of beam elements with axial stress. (If none, leave a blank card)

B2: (I4, F16.7)

Columns 1 - 4 Beam element number.

5 - 20 Axial stress in the element.

11. Plane stress analysis

If NDI $\leq$ 0 no card is required; otherwise, the following cards should be punched:

A - Identification card (A_6, I4)

Columns 1 - 6 The word LOADIN.

7 - 10 Number of nodal point which have concentrated loads.

B - Inplane nodal point loads (I_4, 2F8.3)

One card is required for each nodal point which has a nodal point load.

Columns 1 - 4 Nodal point number.

5 - 12 Load in the x - direction.

13 - 20 Load in the y - direction.

No load can be specified at any nodal point which is fixed against inplane displacements.

12. Plate bending analysis

If ND2 $\leq$ 0 no card is required, otherwise the following cards should be punched:

A - Identification card (A6, $2I_4$)

Columns 1 - 6 The word LOADPB.

7 - 10 Number of nodal points which are loaded with nodal point forces or moments.

11 - 14 (NLD) Parameter defining type of the distributed load:
= 0, if no distributed load is present.
= 1, if the intensity of the distributed load for each corner of the quadrilateral field is to be read in. (This option can be only used when the quadrilateral mesh is generated.)
= 3, if the intensity of the distributed load for each nodal point is to be read in.

B - Nodal point Loads (I_4, 6x, 3F10.3)

One card is required for each nodal point which is loaded with transverse force or moment.

Columns 1 - 4 Nodal point number.

11 - 20 Load in the z - direction.

21 - 30 Moment in the direction of θ_x rotation.

31 - 40 Moment in the direction of θ_y rotation.

C - Corner point values of the distributed load (4I0.3)

No card is required if NLD ≠ 1, otherwise one card should be punched:

Columns 1 - 10 Intensity of the distributed load at the corner 1.

11 - 20 Same for corner 2.

21 - 30 Same for corner 3.

31 - 40 Same for corner 4.

D - Nodal point values of the distributed load (8F10.3)

No card is required if NLD ≠ 3. Otherwise, values of the distributed load at the nodal points should be punched in sequence of nodal point numbering. Eight values should be punched on each card.

13. Plate buckling analysis

No card is required if ND2 ≠ 0. Otherwise two cards should be punched:

A - Control Card (I4, F10.3)

Columns 1 - 4 Number of loads which are applied to the structure to excite the initial mode shapes.

5 - 14 Initial shift used in inverse iteration (estimate for the buckling eigenvalue). If no estimate is available, set this number equal to zero.

B - Nodal point loads (I4, F10.3)

For each nodal point with transverse load (to excite

the initial mode shape) one card is required. Moments are not allowed.

Columns 1 - 4 Nodal point number.

5 - 14 Transverse load.

Note that the excited mode shape should include both symmetric and anti-symmetric components.

14. STOP card (A6)

If the job is to be terminated the word STOP should be punched in columns 1 - 5. Otherwise, a new problem can be initiated by punching a START card.

IV. Numerical Examples

Summary of Cases Considered

Several simple numerical examples were solved first in order to test the different parts of the computer program and to compare the results with exact solutions or solutions obtained by other methods. A number of more complex problems were then solved to demonstrate the capabilities of the computer program.

A comparison was made between the triangular and quadrilateral plate bending elements for an isotropic plate under uniformly distributed load. The loading was presented in two different ways, as equivalent point loads and as consistent nodal point forces and moments. A convergence test for the orthotropic plate bending element, as the number of finite elements increased, was carried out. The solution was compared with a series solution given in [3]. The buckling of a simply supported plate and also the bending of a plate under combined inplane and lateral loads were examined, in order to test the geometric stiffness matrix.

Next, the slightly more complicated problem of stability of a longitundinally stiffened plate field was solved. This example corresponds to the buckling of the deck of a ship between transverse girders. Depending on the stiffness of the stiffeners relative to that of the plate, one may find two different modes of buckling: i) local plate buckling, ii) buckling of plate and stiffeners together. The bending of a stiffened plate field corresponding to a transversely framed ship, was studied and the additional stresses and displacements due to the presence of inplane loads were demonstrated. Buckling of an orthogonally stiffened plate field was examined.

Results of different idealizations were compared. Finally the buckling of a stiffened girder web was dealt with. For this problem, the full capabilities of the computer program were used. The plane stress problem was first solved to compute the geometric stiffness matrix; then the eigenvalue problem was solved to find the buckling load. Each of these cases is discussed briefly in the following sections.

1. Comparison between elements.

A quarter of a square plate, i) simply supported, ii) clamped along the boundary is analyzed. The plate is idealized by a finite element mesh of, a) 9 quadrilateral elements, b) 18 triangular elements, c) 36 triangular elements. The results found by the finite element analysis are compared with exact results in Table 1. The uniformly distributed load has been represented in two different ways: i) by equivalent nodal point forces, ii) by consistent nodal point forces and moments as derived by Zienkiewicz in [6], page 98.

From these extremely simple examples some interesting information can be found. For a uniformly distributed load the consistent nodal point moments from adjacent elements will cancel everywhere except along a boundary which is free to rotate. Consequently for the clamped plate there is no difference between nodal point forces and consistent loading.

For the same number of nodal points, the quadrilateral elements give more accurate results than the triangular elements. To idealize a complex geometry (for example cutouts in a plate) and to obtain a refined mesh in a subregion, the triangular elements may be quite useful--but their use should be kept to a minimum for maximum accuracy.

Table 1. - Results for an Isotropic Plate Loaded by a Uniformly Distributed Load.

Finite Element Idealization	Boundary Condition	Representation of Load	Deflection at Center		Bending Moment at Center		Twisting Moment at Corner	
	C = Clamped SS = Simply Supported	C = Consistent P = Point Load	$\alpha \cdot 10^6$	% error	$\beta \cdot 10^5$	%error	$\gamma \cdot 10^5$	%error
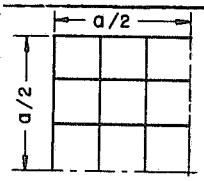	C	P C	1230 1230	-2.4 -2.4	2210 2190	-4.3 -5.2		
	SS	P C	3838 4006	-5.5 -1.4	4502 4622	-6.0 -3.5	2846 3096	-12.3 - 4.6
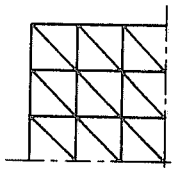	C	C	1190	-5.6	2350	1.7		
	SS	C	3967	-2.3	4594	-4.1	3299	1.6
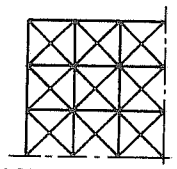	C	C	1210	-4.0	2230	-3.5		
	SS	C	4005	-1.4	4728	-1.3	3092	- 4.8
Analytical Solution	C		1260		2310			
	SS		4062		4789		3246	

$t/a = 1/12$, $\nu = 0.3$, $D = \dfrac{Et^3}{12(1-\nu^2)}$

$W_c = \alpha \cdot q\, a^4/D$ (Deflection at center of plate)

$M_{bc} = \beta \cdot q\, a^2$ (M_{xx} and M_{yy} at center of plate)

$M_{tc} = \gamma \cdot q\, a^2$ (M_{xy} at corner of plate)

t = plate thickness

q = intensity of the uniform lateral load

E = modulus of elasticity

ν = Possion's ratio

a = plate side

The deflections are generally more accurate than the bending moments. The reason for this is that the bending moments are derived from the curvature which is the second derivative of the displacements. It may also be noted that the simply supported boundary condition gives better results than the clamped boundary. This is also well known from the series solution, and is due to the fact that the clamped case is not so well approximated by simple polynomials and trigonometric functions.

2. Convergence of the Orthotropic Plate Element

The orthotropic plate element differs from the isotropic only in the moment curvature relationship:

$$\{M\} = [D]\{X\}$$

For an isotropic plate

$$[D] = \frac{E\,t^3}{12\,(1-\nu^2)} \begin{bmatrix} 1 & \nu & 0 \\ \nu & 1 & 0 \\ 0 & 0 & \frac{1-\nu}{2} \end{bmatrix}$$

For a general orthotropic plate six constants are required to define the symmetric[D]matrix:

$$[D] = \begin{bmatrix} D_1 & D_4 & D_5 \\ D_4 & D_2 & D_6 \\ D_5 & D_6 & D_3 \end{bmatrix}$$

For an orthotropic plate with elastic axes coinciding with the coordinate axes the matrix is somewhat simpler ($D_5 = D_6 = 0$, $D_1 = D_x$, $D_2 = D_y$, $D_3 = D_{xy}$). The finite element solutions for orthotropic plates with data as given in Fig. 7 and Table 2, were compared with series solutions presented by Mansour [3]. Note that in this table: $H = D_4 = 2D_{xy}$. As will be seen in Table 2 and also in

Table 2 - Results for a Simply Supported Orthotropic Plate Loaded by a Uniformly Distributed Load.

$\zeta = \frac{a}{b}\sqrt{\frac{D_x}{D_y}}$	$\eta = \frac{H}{\sqrt{D_x D_y}}$	Solution Method	Mesh Size	Deflection at Center		Bending Moment M_{xx} at Center		Bending Moment M_{yy} at Center	
				$\alpha.10^5$	% difference	$\beta.10^5$	% difference	$\gamma.10^4$	% difference
2	0.5	Finite Element	2x2	1179	-1.9	1820	-8.2	1128	-2.1
			4x4	1197	-0.42	1930	-2.0	1147	-0.3
		Series		1202	0	1969	0	1151	0
2	1	Finite Element	1x1	952	-6.1	2700	55.0	882	-8.5
			2x2	992	-2.1	1620	-6.9	943	-2.3
			4x4	1008	-0.45	1707	-1.9	960	-0.47
			6x6	1011	-0.20	1725	-0.85	963	-0.20
		Series		1013	0	1741	0	965	0

$W_c = \alpha \cdot q\, b^4/D_y$ (Deflection at center of plate)

$M_{xc} = \beta \cdot q\, b^2 \sqrt{D_x/D_y}$ (M_{xx} at center of plate)

$M_{yc} = \gamma \cdot q\, b^2$ (M_{yy} at center of plate)

q = intensity of the uniform lateral load

a = plate length

b = plate width

D_x, D_y and H are defined on page 31

Note: The indicated finite element meshes correspond to a quarter of the plate.

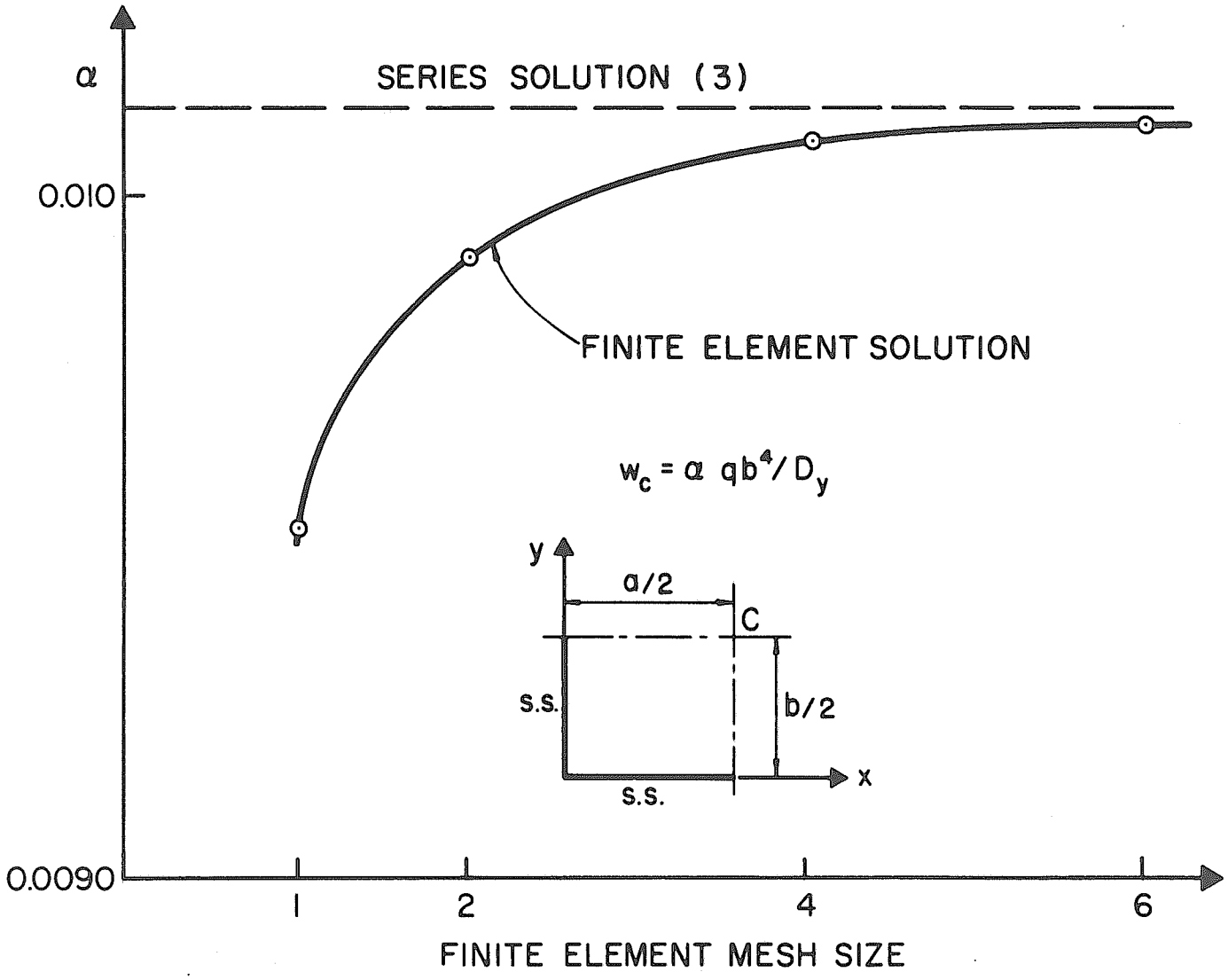

FIG. 7 CONVERGENCE OF FINITE ELEMENT SOLUTION FOR A SIMPLY SUPPORTED ORTHOTROPIC PLATE

Fig. 7, excellent agreement was found between results by the two different methods. As mentioned proviously, the finite elements used in the program are compatible. For the plate bending elements this means that deflections and slopes are continuous between two adjacent elements. These elements will give a uniform convergence of displacement towards the exact solution as the mesh is refined, always on the stiffer side. This is clearly demonstrated in Fig. 7. One important point should be mentioned about the comparison between the finite element and series solutions. While the plate selected for the purpose of comparison is of extremely simple geometrical shape, plates of completely arbitrary shape, for example cutouts, can be idealized by finite elements and the distribution of displacements and stresses over the entire field can be found. The series analysis cannot be applied for such general cases.

3. Test of Geometric Stiffness

The geometric stiffness matrix with a cubic expansion for w as derived in Appendix A has been tested extensively and found to give satisfactory results. Here two extremely simple examples will be given to demonstrate the use of the geometric stiffness. A simply supported plate shown in Fig. 8 is subjected to an inplane load $\sigma_x = 5000\ lb/in^2$.

The buckling problem as given by Eq. (11) is to determine the ratio λ by which the inplane load can be increased before the plate becomes unstable. The buckling stress is then given by:

$$\sigma_{cr} = \lambda\, \sigma_x$$

The analytic expression for the buckling stress is:

$$\sigma_{cr} = \frac{\pi^2 E}{12(1 - \nu^2)} \left(\frac{t}{a}\right)^2 \cdot 4$$

Inserting numerical values, a = 12 in., t = .12 in. and E = 3 x 10^7 lb/in^2, in this expression yeilds:

$$\sigma_{cr} = \underline{10{,}840 \text{ lb/in}^2}$$

A quarter of the plate was divided into a 3 x 3 mesh of quadrilateral finite elements and the program was used to solve the buckling problem. The following result was found:

$$\lambda = \underline{2.199}$$

$$\sigma_{cr} = 2.199 \text{ X } 5000 = 10995 \text{ lb/in}^2$$

This corresponds to an error of 1.5%. Since the stiffness is over-estimated by the finite element method, the computed result for the buckling load is higher than the exact one. Alternatively, the problem of a plate under combined inplane and lateral load can be solved. This problem is frequently encountered in ship structures, for example in bottom plating.

Even for this extremely simple problem no analytic closed form solution exists. A first order approximation can be made using the so-called magnification factor m, to estimate values of displacement w and moment M in some special cases:

$$m = 1/(1 - \sigma/\sigma_{cr})$$

$$w = w_o m$$

$$M = M_o m$$

where w_o and M_o are deflection and moment found when no inplane loads are present.

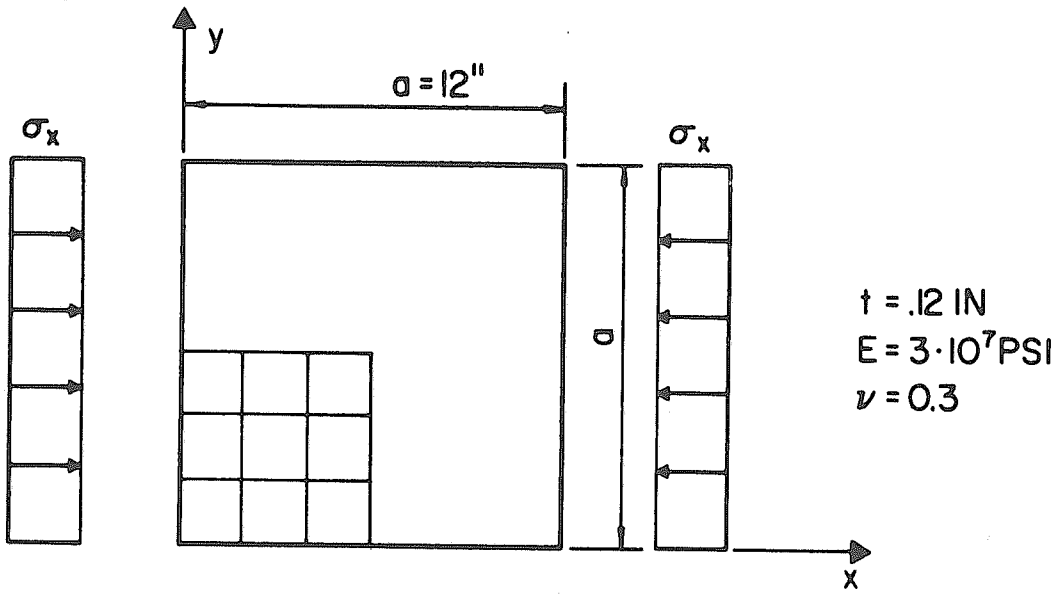

FIG. 8 SIMPLY SUPPORTED PLATE UNDER UNIFORM INPLANE LOAD σ_x

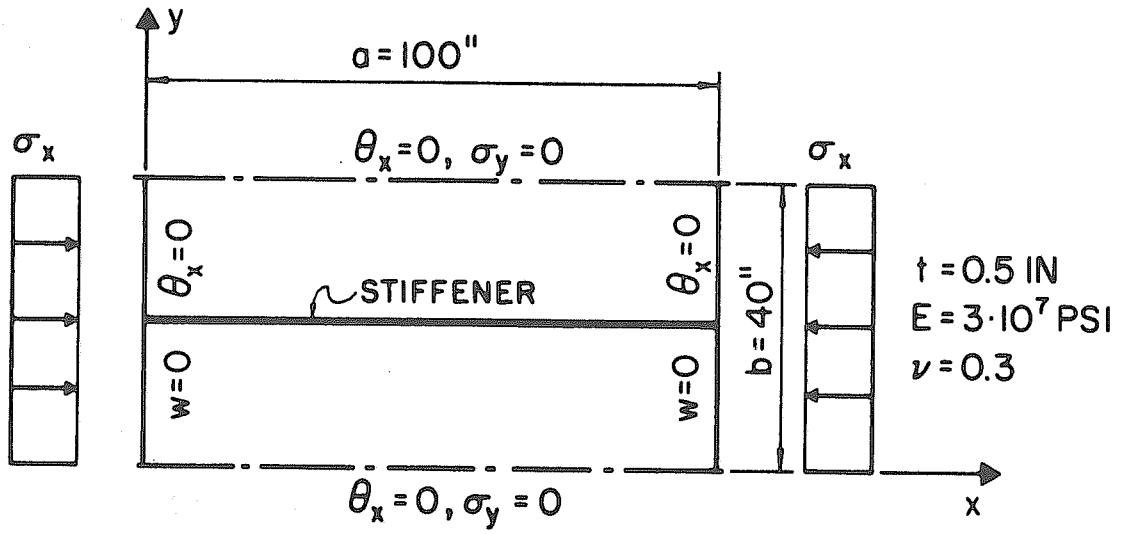

FIG. 9 SIMPLY SUPPORTED PLATE WITH LONGITUDINAL STIFFENERS

As an example, the simply supported square plate of the previous example with the same inplane loading was examined. The plate was assumed to be subjected to uniform lateral pressure of intensity $q = 1\ lb/in^2$ and the deflection and the bending moment at center of the plate were calculated:

$$m = 1/\left(1 - \frac{5000}{10840}\right) = 1.856$$

$$w_c = 0.00406 \cdot (q\ a^4/D) \cdot m = 0.0330\ in$$

$$M_c = -0.04789 \cdot q\ a^2 \cdot m = -12.80\ lb.in/in$$

Using the same mesh as in the previous example, the finite element method gives the following results:

$$\bar{w}_c = 0.0310\ in$$

$$\bar{M}_c = -12.33\ lb.in/in$$

This is considered to represent excellent agreement.

4. Buckling of a Plate with Longitudinal Stiffeners

The plate with longitudinal stiffeners shown in Fig. 9 corresponds to the deck of a longituninally stiffened ship. Depending on the relative stiffness of the stiffeners with respect to the stiffness of the plate one obtains primary buckling of the plate and the stiffeners or local buckling of the plate between the stiffeners. Both these cases will be considered by choosing two different stiffener types:

a) $A_{st} = 1\ in^2$, $I_{st} = 8.33\ in^4$ Primary buckling

b) $A_{st} = 1.4\ in^2$, $I_{st} = 22.87\ in^4$ Local plate buckling

where A_{st} and I_{st} are cross-sectional area and moment of inertia

of the stiffeners, respectively. Two different meshes were used for both these cases, Mesh 1 is a 4 x 6 mesh for the whole field, while Mesh 2 is a 4 x 12 mesh for one quarter of the plate field. Since one does not generally know, a priori, the buckled shape, a crude mesh including the whole field is required for the first analysis. Later a more accurate solution can be found by a finer mesh taking advantage of symmetry.

For case a, Reference 12 gives the following result from an approximate solution: $\sigma_{cr} = 11.70$ lb/in^2. The solutions by the finite element program are:

$$\bar{\sigma}_{cr} = 11.64 \text{ lb/in}^2 \qquad \text{(Mesh 1)}$$

$$\bar{\sigma}_{cr} = 11.58 \text{ lb/in}^2 \qquad \text{(Mesh 2)}$$

For case b, one may find an exact solution if the stiffeners are given no torsional rigidity. The buckled shape will have node lines along the stiffeners, so the problem is reduced to the buckling of an unstiffened plate.

The analytical solution of the problem gives:

$$\sigma_{cr} = 17.53 \text{ lb/in}^2$$

The finite element results are

$$\bar{\sigma}_{cr} = 18.98 \text{ lb/in}^2 \qquad \text{(Mesh 1)}$$

$$\bar{\sigma}_{cr} = 17.91 \text{ lb/in}^2 \qquad \text{(Mesh 2)}$$

Actually, the exact solution for this problem has three halfwaves in the longitudinal direction, while the finite element program gives two. This difference is probably due to the fact that the initial shape was closer to the two half-wave solution than to the other one. The analytical solution corresponding to two halfwaves

is σ_{cr} = 17.82 lb/in^2 so the two solution are quite close. In Fig. 10 and Fig. 11, the plots of the buckled shape for cases a and b, as printed by the computer program, are shown.

For the practical use of the finite element program in solving buckling problems two points should be emphasized.

1. An initial static load must be given. The corresponding displacements should not be symmetric or antisymmetric. The reason for this is that if the initial vector in the inverse iteration corresponds to a symmetric buckled shape, but the real buckled shape is anti-symmetric, the computer algorithm will not converge. In the example 4, the initial shape was symmetric and anti-symmetric for cases a and b, respectively.

2. To improve the speed of convergence an initial shift μ lower than the expected eigenvalue λ can be read in. Under no circumstances may a shift higher than the lowest eigenvalue be given. In that case the computer algorithm may converge to a different buckled shape which does not correspond to the correct solution. As explained earlier a shift μ speeds up the convergence, but to be on the safe side, $\mu = 0$, should be used where no safe estimate of the buckling load is available.

5. Transversely Stiffened Plate Under Combined Inplane and Lateral Loads.

This example corresponds to the bottom plating of a transversely framed ship and demonstrates the effect on the plate bending behavior of the inplane stresses. As shown in Fig. 12, a plate with an infinite number of transverse stiffeners is assumed to be subjected to combined inplane and lateral loads. The plate-stiffener combination is assumed to be clamped along its longitudinal edges. Two different

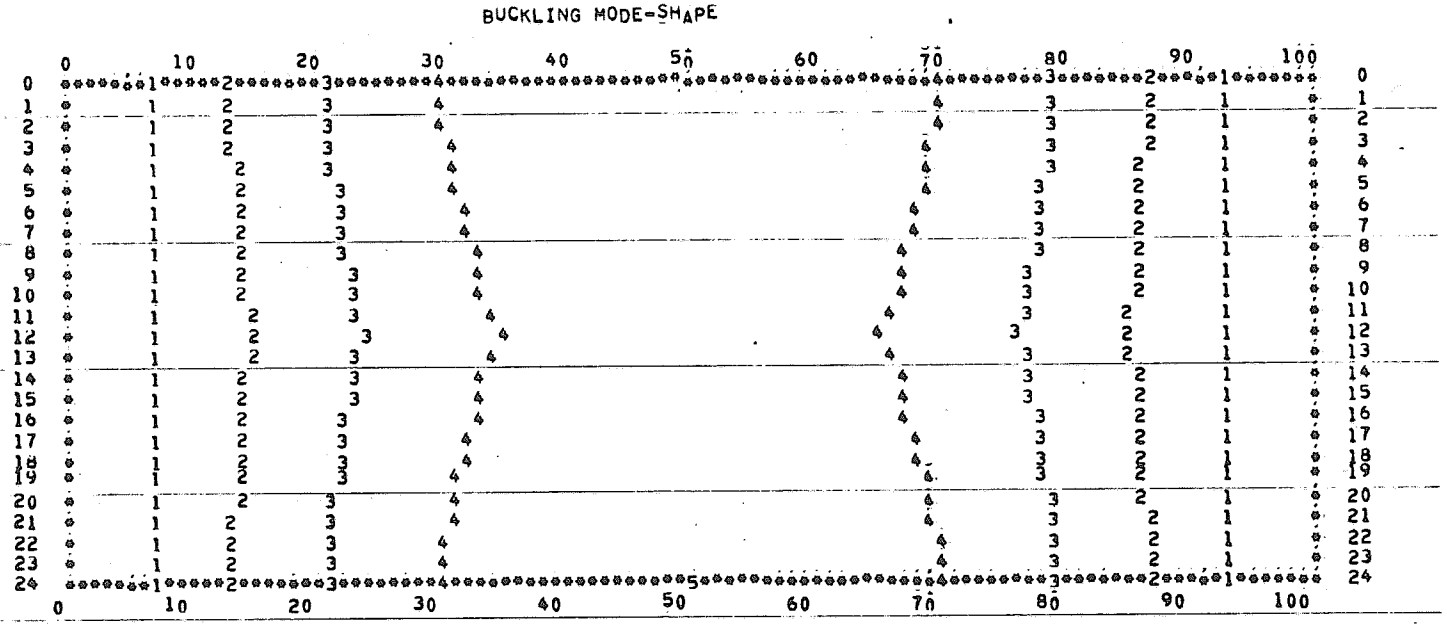

REFERENCES

LINE SYMBOL	VALUES	
0	0.	-0.
1	.200000	-.200000
2	.400000	-.400000
3	.600000	-.600000
4	.800000	-.800000
5	1.000000	-1.000000
6	1.200000	-1.200000
7	1.400000	-1.400000
8	1.600000	-1.600000
9	1.800000	-1.800000
D	2.000000	-2.000000
*	BOUNDARY POINTS	

TIME FOR COMPLETE ANALYSIS IN SECONDS 22.344

FIG.10 BUCKLED SHAPE OF THE PLATE WITH LONGITUDINAL STIFFENERS (CASE a, MESH 1)

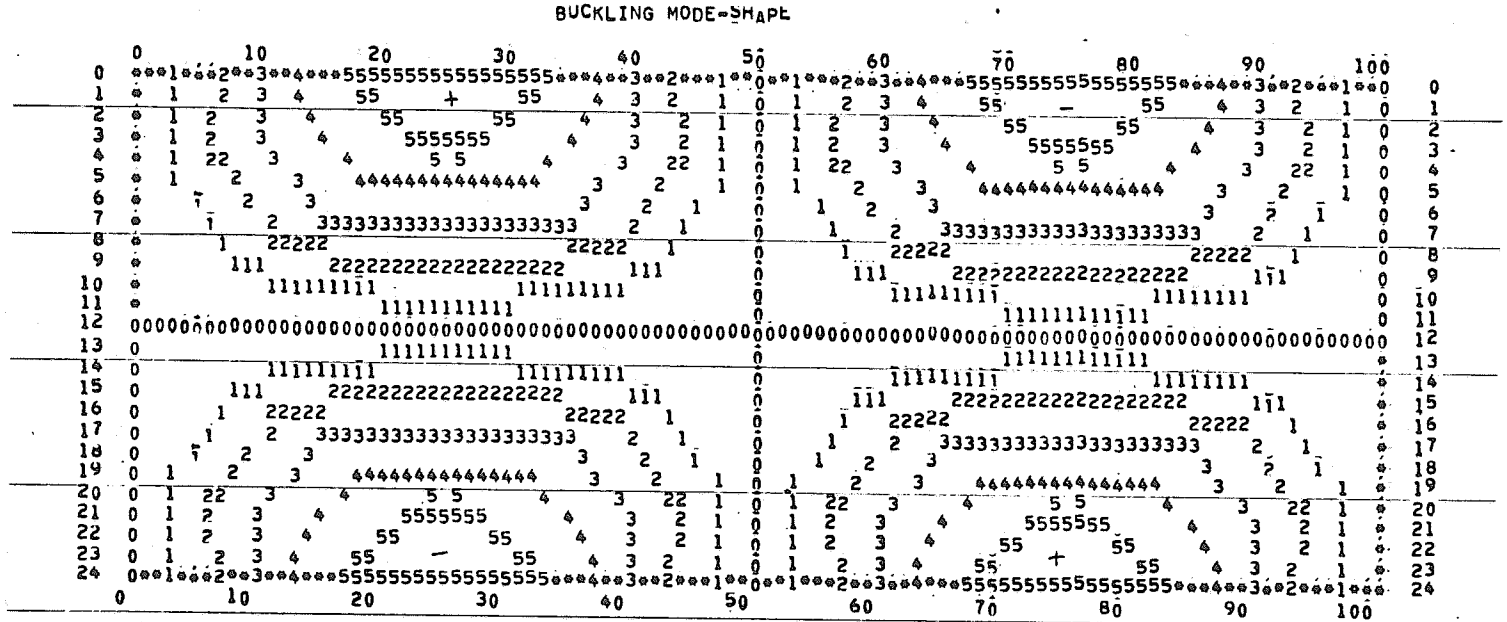

FIG. 11 BUCKLED SHAPE OF THE PLATE WITH LONGITUDINAL STIFFENERS
(CASE b, MESH 1)

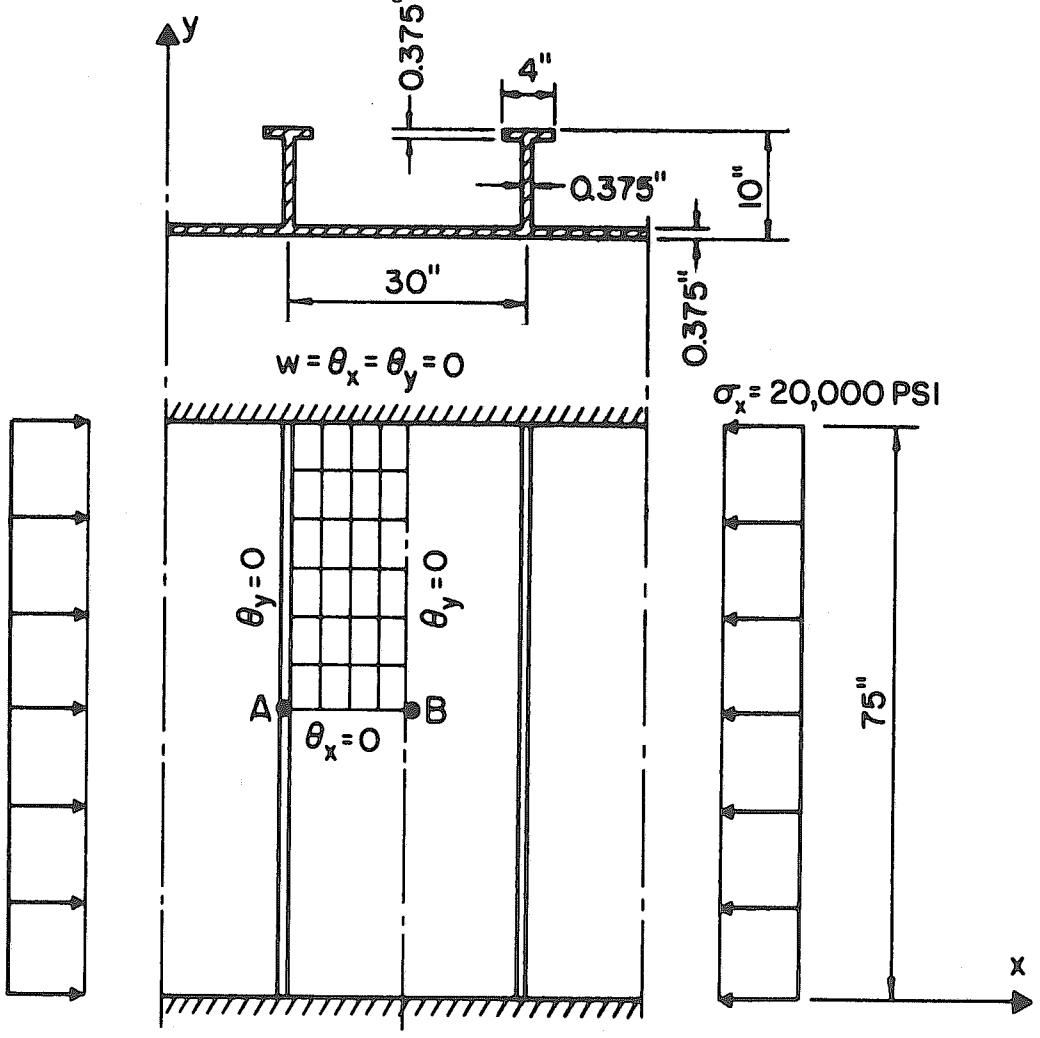

E = 3·10 PSI , ν = 0.3

FIG. 12 TRANSVERSALLY STIFFENED PLATE UNDER COMBINED INPLANE AND LATERAL LOADS, σ_x = 20,000 PSI, q = 17.3 PSI

idealizations were made to obtain the finite element solution of this problem:

1. The stiffeners were assumed to be rigid, i.e., an individual plate panel was assumed to be clamped along its boundary. If a plate strip, perpendicular to the stiffeners, is considered at the middle of the plate, the deflection w at its center and the bending moment M_x at its center and ends can be approximately calculated by the beam-column theory [13]. Thus, in this case, the finite element results can be directly compared with those of the analytical solution.
2. The effect of flexible stiffeners supporting the plate panels was included.

Both analytical and finite element results are presented in Table 3. As can be seen the moments are not very much affected by assuming the stiffeners to be rigid. The agreement between analytical and finite element results is again very satisfactory. The computer plots of deflections and moments in one quarter of a plate panel is shown in Figs. 13, 14, 15 and 16. These plots correspond to the case when the stiffeners are assumed to be flexible.

6. Buckling of an Orthogonally Stiffened Plate Field

This example demonstrates how the actual physical problem can be idealized in different ways when using the finite element method of analysis. Three different representations of the plate field shown in Fig. 17 were tried:

a) The stiffened plate was idealized as an orthotropic plate. The stiffness of the stiffeners was uniformly distributed in both directions.

Table 3 - Numerical Results for Transversely Stiffened Plate

	(1) Plate Under Lateral Load Only	(2) Magnification factor m	Plate Under Combined Loads (1)x(2)	Finite Element Results	
				Transverse Stiff. Rigid	Transverse Stiff. Flex.
w at point B	0.0311	1.413	0.0439	0.0436	0.0500
M_{xx} at point B	-646	1.488	-962	-975	-976
M_{xx} at point A	+1294	1.270	1642	1627	1613

Note: Units are lb and lb. in.

Table 4 - Numerical Results for Orthogonally Stiffened Plate

Idealization	Mesh for Complete Field	Buckling Stress (psi)	Difference % to lowest
a	9 x 6	34.94	11.0
	20 x 12	34.21	8.5
b	9 x 6	32.60	3.4
c	9 x 6	32.23	2.2
	18 x 12	31.59	0.2
	18 x 18	31.53	0
Orthotropic Plate Theory Solution		33.60	6.6

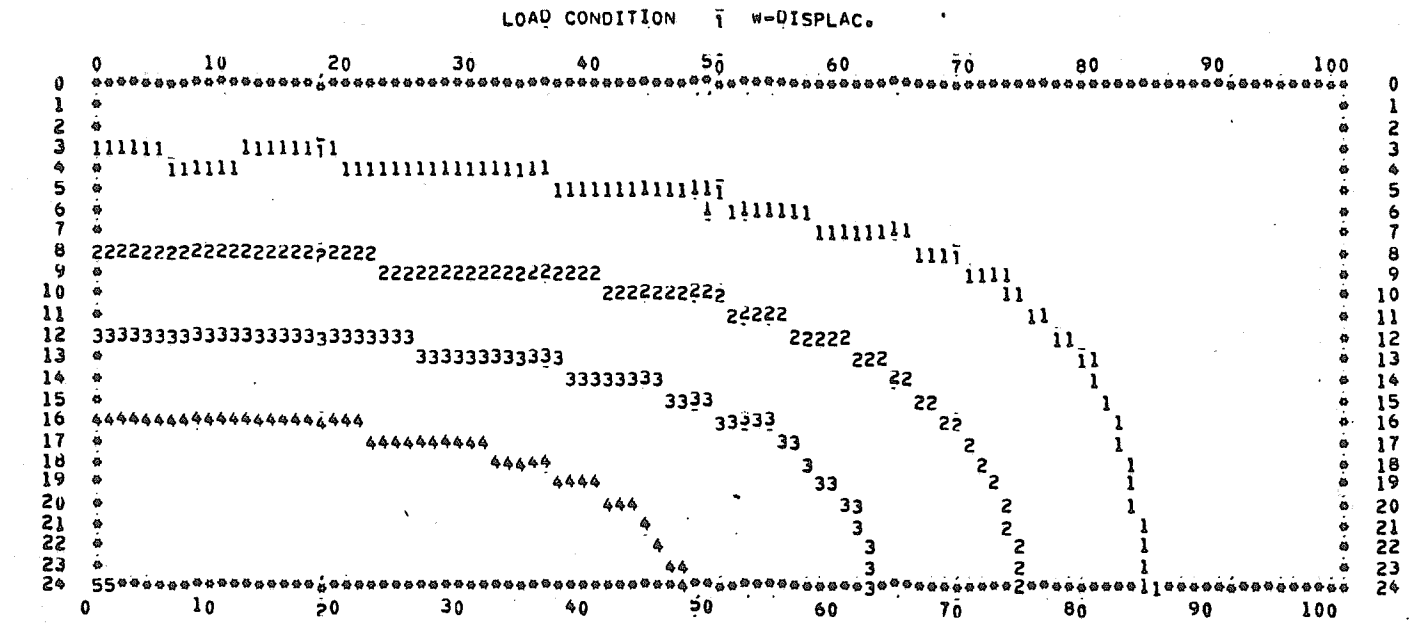

FIG.13 DEFLECTED SHAPE OF THE TRANSVERSELY STIFFENED PLATE UNDER COMBINED LOADS

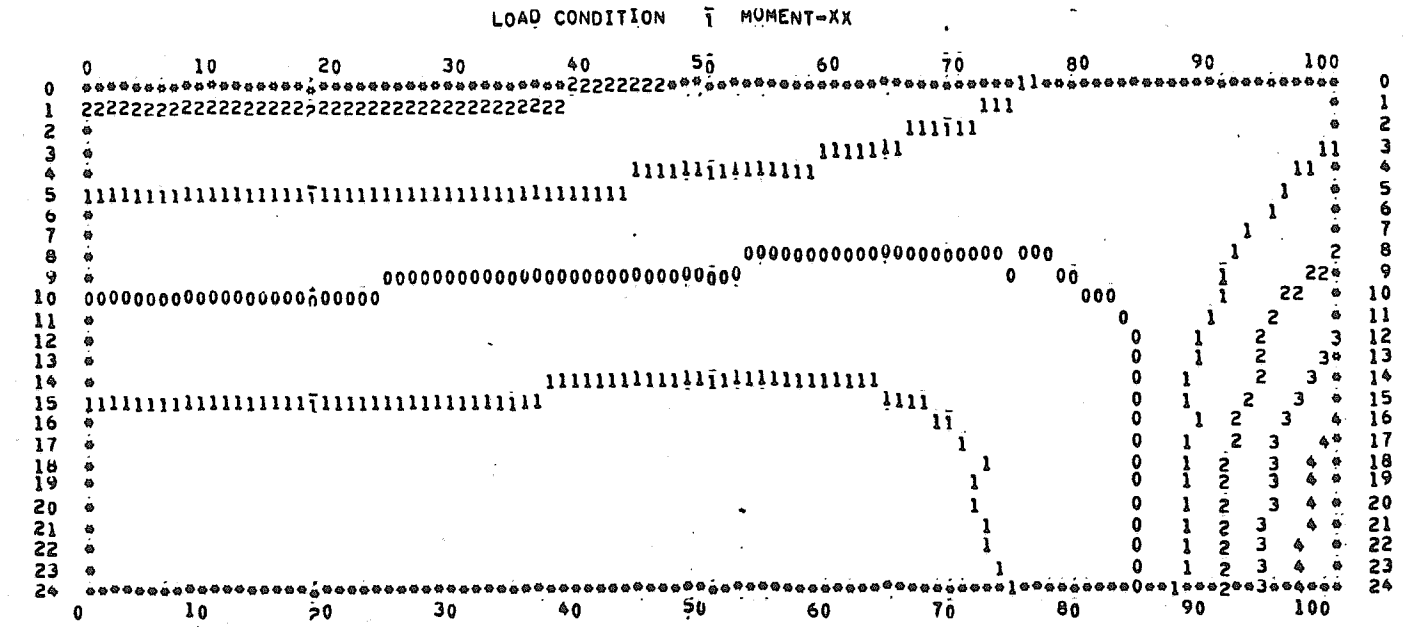

REFERENCES

LINE SYMBOL VALUES

0	0.	-0.
1	200.000000	-200.000000
2	400.000000	-400.000000
3	600.000000	-600.000000
4	800.000000	-800.000000
5	1000.000000	-1000.000000
6	1200.000000	-1200.000000
7	1400.000000	-1400.000000
8	1600.000000	-1600.000000
9	1800.000000	-1800.000000
D	2000.000000	-2000.000000
*	BOUNDARY POINTS	

FIG.14 BENDING MOMENT M_{xx} OF THE TRANSVERSELY STIFFENED PLATE UNDER COMBINED LOADS

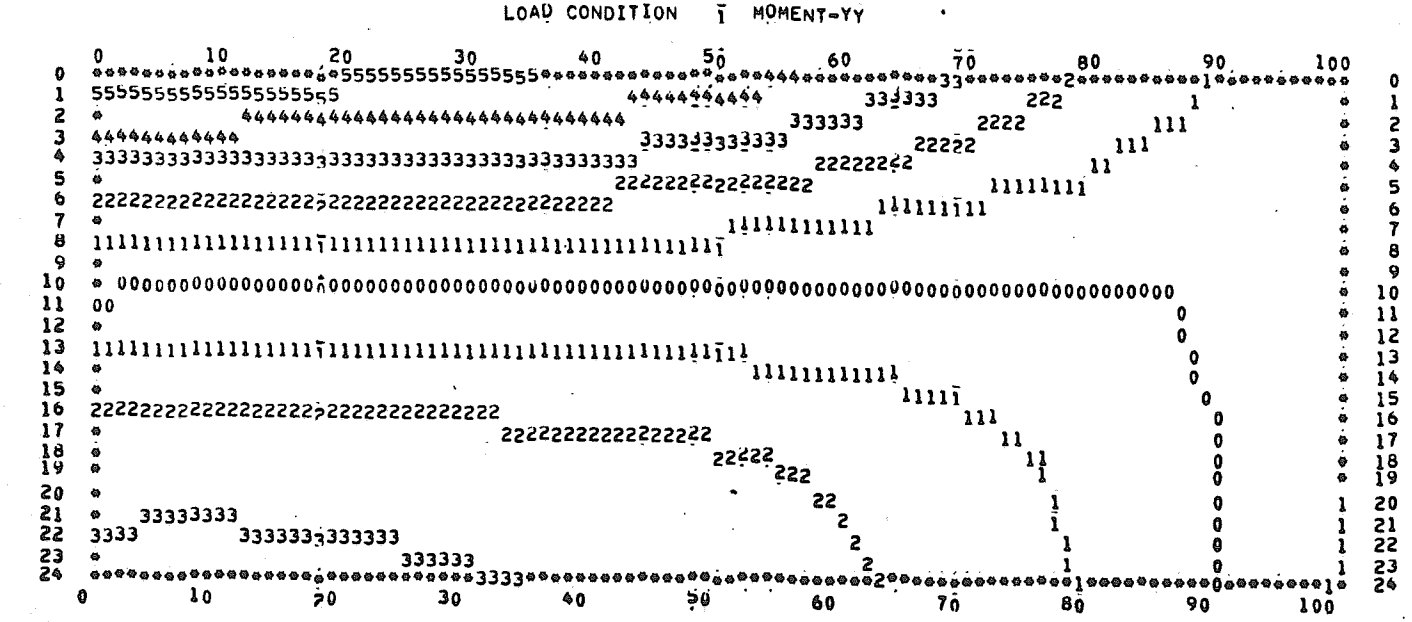

REFERENCES

LINE	SYMBOL	VALUES	
0		0.	-0.
1		300.000000	-300.000000
2		600.000000	-600.000000
3		900.000000	-900.000000
4		1200.000000	-1200.000000
5		1500.000000	-1500.000000
6		1800.000000	-1800.000000
7		2100.000000	-2100.000000
8		2400.000000	-2400.000000
9		2700.000000	-2700.000000
D		3000.000000	-3000.000000
*		BOUNDARY POINTS	

FIG. 15 BENDING MOMENT M_{yy} OF THE TRANSVERSELY STIFFENED PLATE UNDER COMBINED LOADS

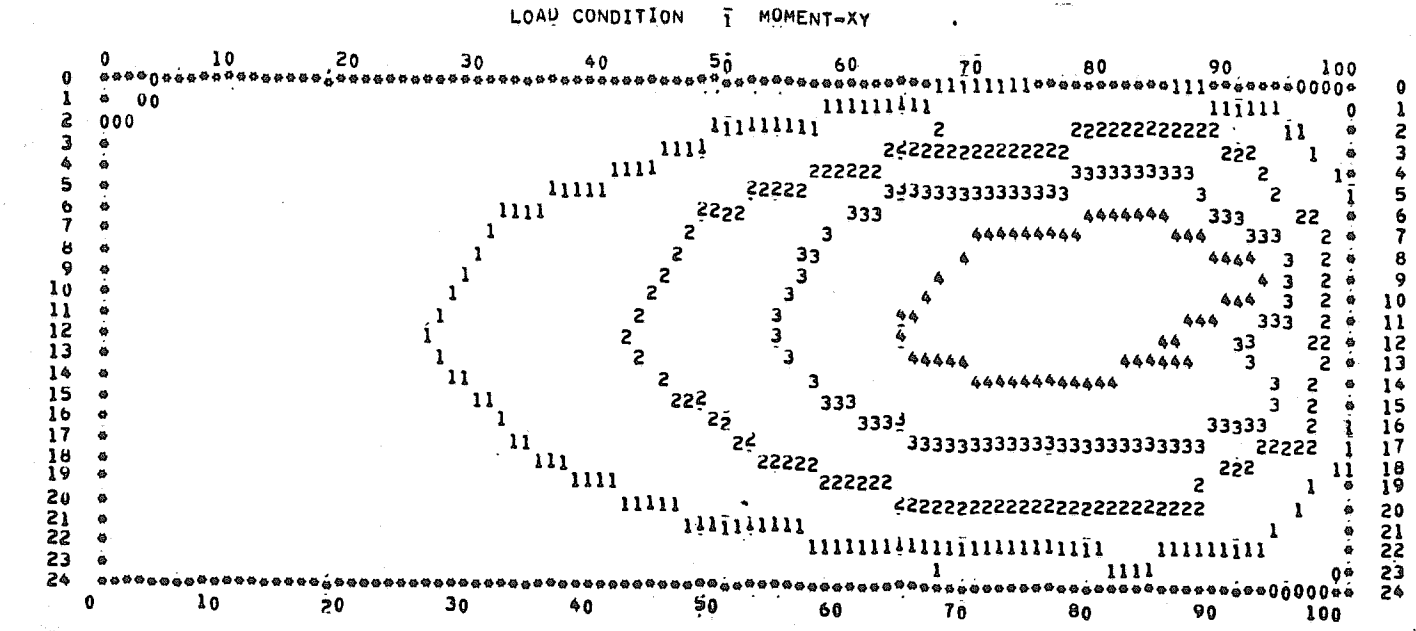

REFERENCES

LINE SYMBOL VALUES

0	0.	-0.
1	40.000000	-40.000000
2	80.000000	-80.000000
3	120.000000	-120.000000
4	160.000000	-160.000000
5	200.000000	-200.000000
6	240.000000	-240.000000
7	280.000000	-280.000000
8	320.000000	-320.000000
9	360.000000	-360.000000
D	400.000000	-400.000000
*	BOUNDARY POINTS	

TIME FOR COMPLETE ANALYSIS IN SECONDS 14.086

FIG.16 TWISTING MOMENT M_{xy} OF THE TRANSVERSELY STIFFENED PLATE UNDER COMBINED LOADS

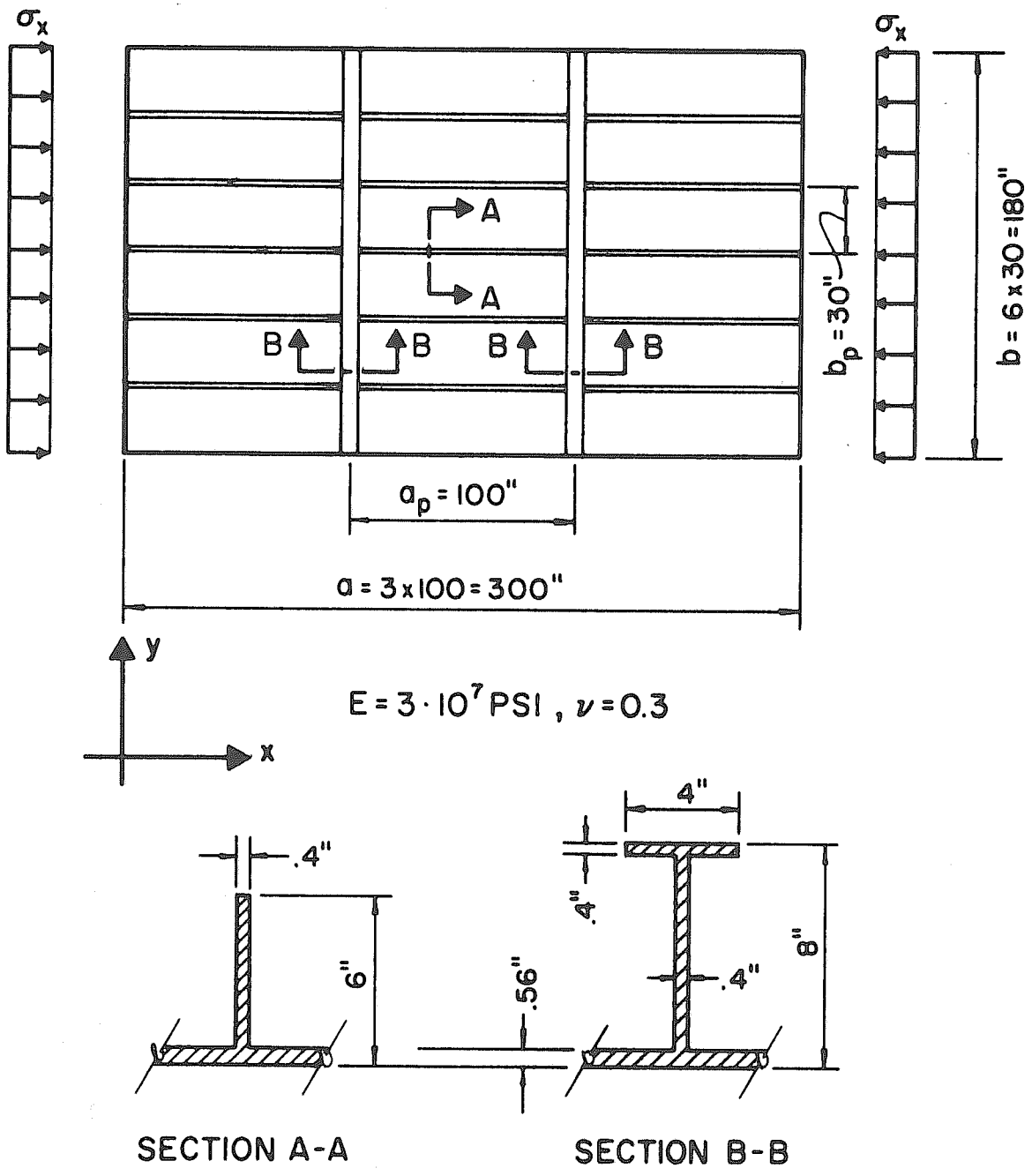

FIG. 17 ORTHOGONALLY STIFFENED PLATE FIELD

b) The stiffness of the longitudinal stiffeners was uniformly distributed, while the transverse supporting girders were represented as discrete beams.

c) Both longitudinal and transverse stiffeners were represented as discrete beams.

In all these cases the effective width of plating was included when computing the moment of inertia of the stiffeners. The numerical results are presented in Table 4 and a plot of the buckled shape for case a is shown in Fig. 18.

Obviously the last idealization is closest to the real structure, but it can be seen that idealization b does not give more than 1.2% difference in the buckling load whereas the idealization a, the orthotropic plate theory solution, overestimates the buckling load by 8.8% (when using 9 x 6 mesh).

As a further check on the finite element results, the buckling load for case a, as obtained by the program, can be compared with that given by the analytical solutions:

$$\sigma_{cr} = \frac{\pi^2}{b^2 (t + t_a)} \left[D_x \left(\frac{mb}{a}\right)^2 + D_y \left(\frac{a}{mb}\right)^2\right]$$

$$D_x = \frac{E I_a (q + 1)}{b} + \frac{E t^3}{12 (1 - \nu^2)}$$

$$D_y = \frac{E I_b (p + 1)}{a} + \frac{E t^3}{12 (1 - \nu^2)}$$

$$t_a = \frac{F_a}{q + 1}$$

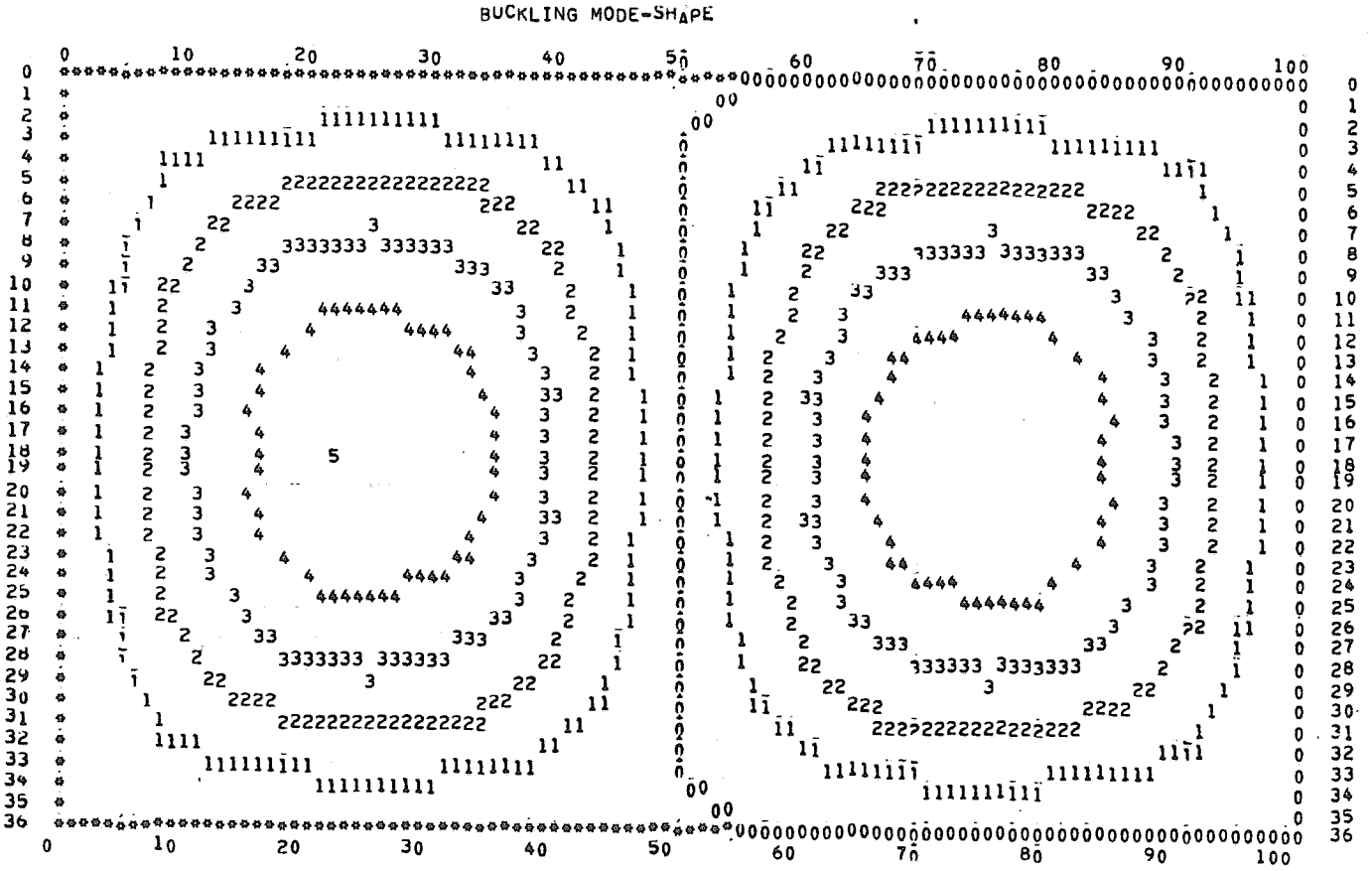

REFERENCES

LINE SYMBOL	VALUES	
0	0.	-0.
1	.200000	-.200000
2	.400000	-.400000
3	.600000	-.600000
4	.800000	-.800000
5	1.000000	-1.000000
6	1.200000	-1.200000
7	1.400000	-1.400000
8	1.600000	-1.600000
9	1.800000	-1.800000
D	2.000000	-2.000000
*	BOUNDARY POINTS	

TIME FOR COMPLETE ANALYSIS IN SECONDS 37.964

FIG.18 BUCKLED SHAPE OF THE ORTHOGONALLY STIFFENED PLATE

$$m = \frac{a}{b} \sqrt[4]{\frac{b\, I_b\, (p + 1)}{a\, I_a\, (q + 1)}}$$

(The calculated value of m should be rounded to an integer number.)

where

F_a = area of longitudinal stiffeners

I_a = moment of inertia of longitudinal stiffeners

I_b = moment of inertia of transverse stiffeners

q = number of longitudinal stiffeners

p = number of transverse stiffeners

a = length of the plate field

b = width of the plate field

t = plate thickness

m = number of halfwaves in the longitudinal direction

The buckling load of the stiffened plate field for case a, evaluated by above formuli, will be:

$$\sigma_{cr} = 33600 \text{ lb/in}^2$$

which is only 1.8% lower than the corresponding finite element solution using the finest mesh. Torsional stiffness was neglected in both finite element and analytical solutions.

7. Buckling of the Stiffened Girder Web

This final example makes use of the complete computer program. The girder which is shown in Fig. 19 corresponds to a transverse girder at the bottom of a tanker. The left side of the girder is clamped whereas the right side is supported by a flexible longitudinal girder. The load is supplied by the reactions of the longitudinal

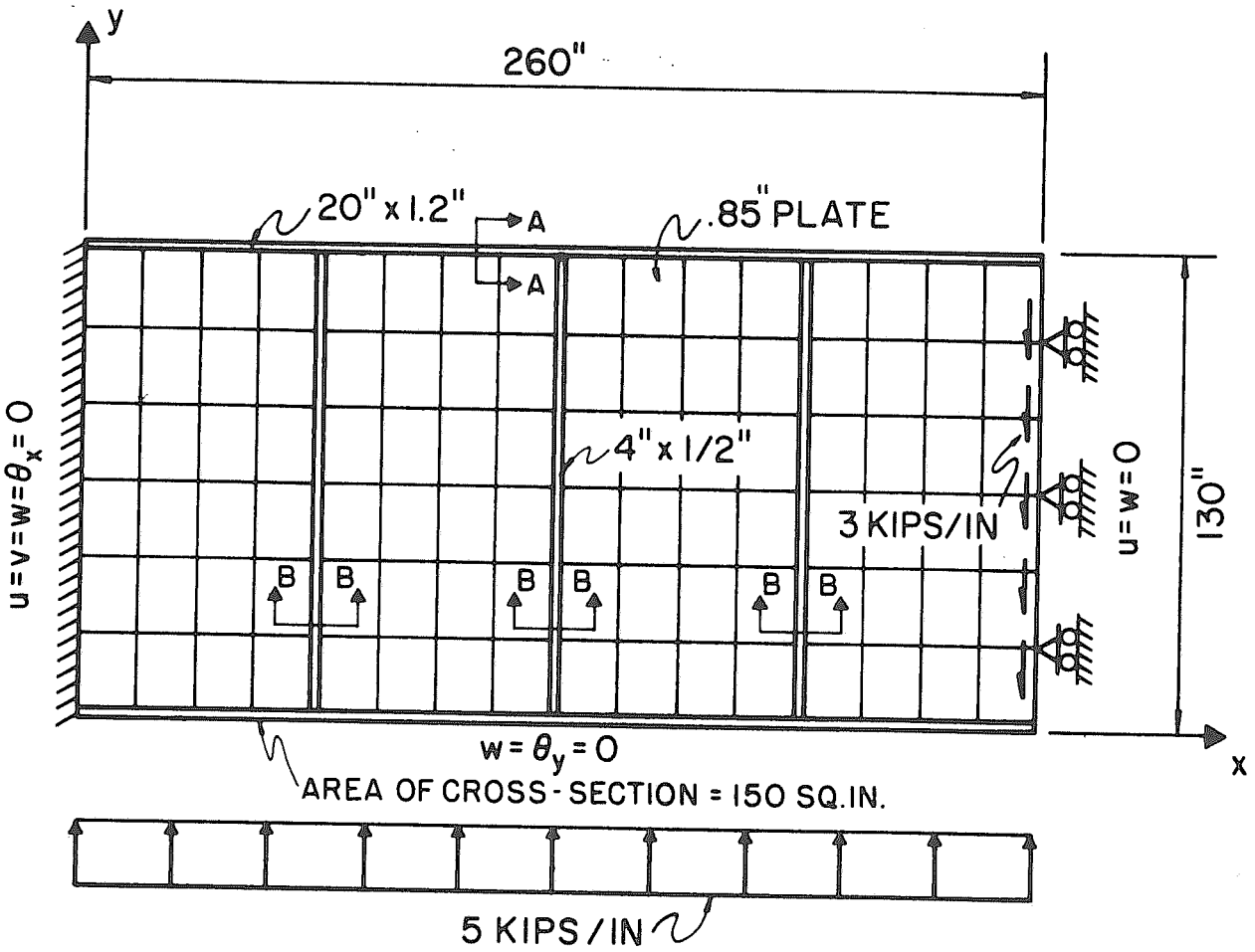

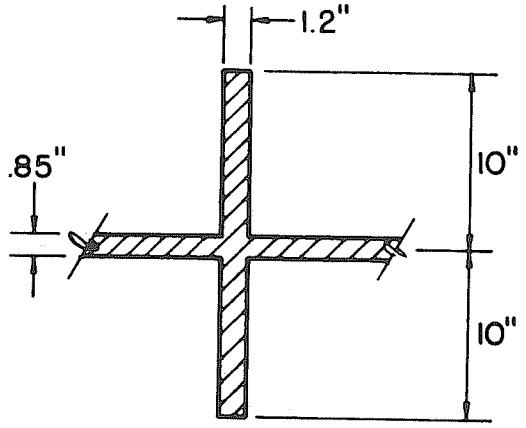

SECTION A-A

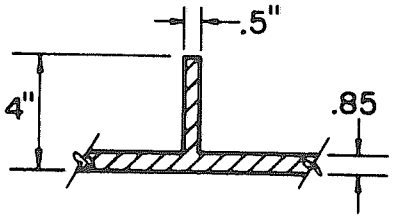

SECTION B-B

FIG. 19 GIRDER WEB, GEOMETRY, LOADING AND FINITE ELEMENT MESH

bottom stiffeners. For this problem, unlike all the previous examples, there is no simple way of finding the inplane stress distribution. Therefore, the plane stress problem was solved by the finite element program as a first step. Then the geometric stiffness matrix of the structure was computed and finally the buckling problem was solved. The plot of the buckled shape, as printed by the computer program is shown in Fig. 20. As expected, the compression zone in the upper part of the web near the clamped edge buckles. The corresponding eigenvalue was found to be $\lambda = 2.47$. This means that with the assumed loading pattern, the loads can be increased by a factor of 2.47 before instability occurs. For this example no analytical solution is available.

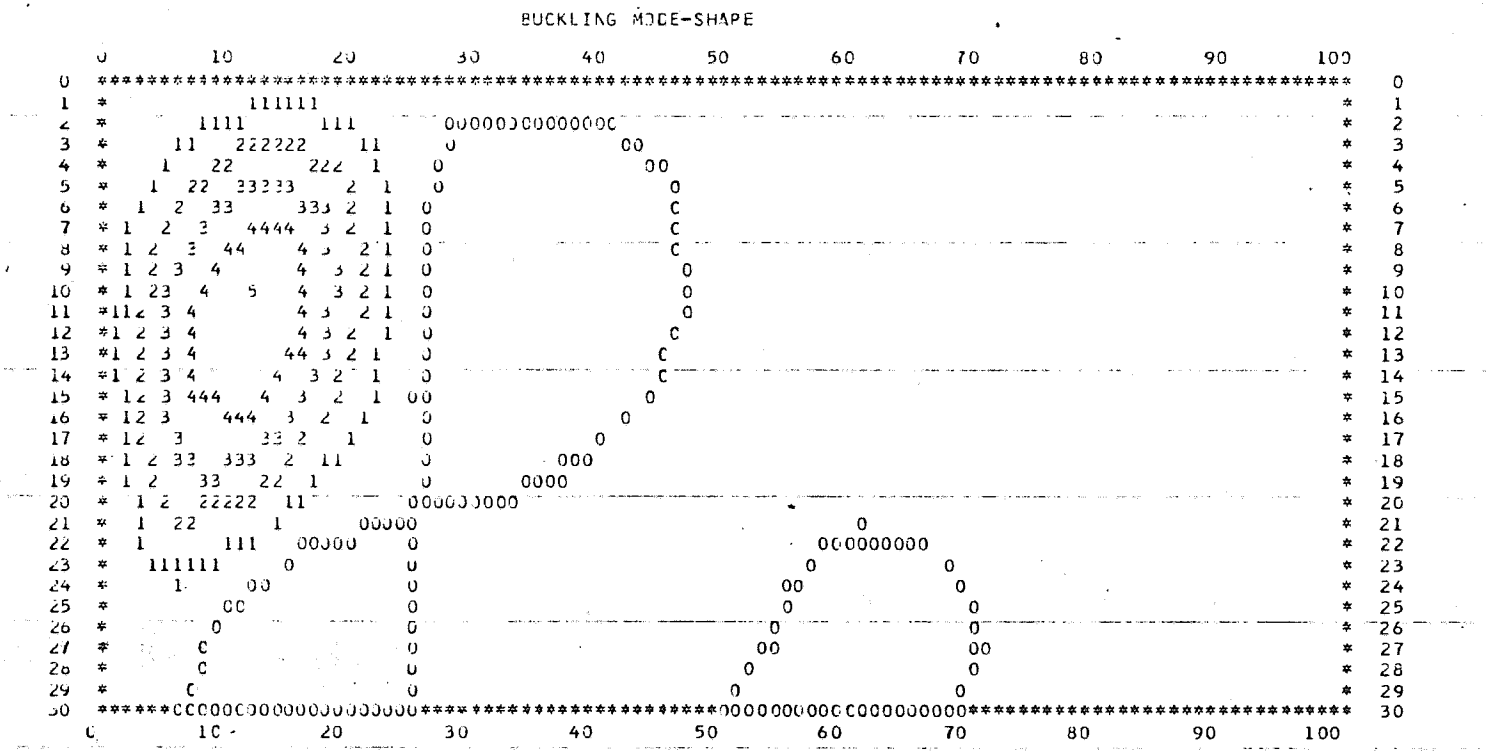

FIG.20 BUCKLED SHAPE OF THE GIRDER WEB

REFERENCES:

1. Clarkson, J., "The Elastic Analysis of Flat Grillages," Cambridge University Press (1965).
2. Schade, H.A., "The Orthogonally Stiffened Plate under Uniform Lateral Load," Trans. ASME, Vol. 62 (Dec. 1940).
3. Mansour, A.D., "Orthotropic Bending of Ship Hull Bottom Plating under Combined Action of Lateral and Inplane Load," University of Calif. Report No. NA-66-2 (1966).
4. Turner, M.J., Clough, R.W., Martin, H.C., and Topp, L.J., "Stiffness and Deflection Analysis of Complex Structures," Journ. Aero. Sci. 23 (1956).
5. Clough, R.W., and Tocher, J.L., "Finite Element Stiffness Matrices for Plate Bending," Conf. on Matrix Meth. in Struc. Mech. AFIT Ohio (1965).
6. Zienkiewicz, O.C., "The Finite Element Method in Structural and Continuum Mechanics," McGraw Hill, London (1967).
7. Clough, R.W., and Felippa, C.A., "A Refined Quadrilateral Element for Analysis of Plate Bending," 2nd Conf. on Matrix Meth. in Struc. Mech. AFIT Ohio (1962).
8. Przemieniecki, J.S., "Theory of Matrix Structural Analysis," McGraw-Hill, New York (1968).
9. Schade, H.A., "The Effective Breadth Concept in Ship Structure Design," Trans. SNAME, Vol. 61, (1953).
10. Gallagher, R. H., and Gellatly, R. A., "A Discrete Element Procedure for Thin Shell Instability Analysis," AIAA Journal Vol. 5, No. 1 (1967).

11. Timoshenko, S. and Woinowski-Krieger, S., "Theory of Plates and Shells,"2nd Ed. McGraw-Hill, New York (1959).

12. Wah, T., "A Guide for the Analysis of Ship Structures," a Government Research Report, U.S. Department of Commerce, Washington, D.C.

13. Timoshenko, S. and Gere, J.M., "Theory of Elastic Stability," 2nd Ed. McGraw-Hill, New York, (1961).

14. Felippa, C., "Refined Finite Element Analysis of Linear and Nonlinear Two-Dimensional Structures," PhD. Thesis, University of Calif., Berkeley (1966).

15. Kapur, K.K., and Hartz, B.J., "Stability of Thin Plates using the Finite Element Method," Proc. ASCE Vol. 92, No. EM-2 (1966).

APPENDIX A

Geometric Stiffness Matrix for the Triangular Plate Bending Element Based on Cubic Interpolation Functions

In the derivation of this geometric stiffness matrix a cubic expansion is used for the transverse displacement w. The same cubic expansion is used by Zienkiewicz [6] in the derivation of a noncompatible triangular plate bending element. The displacement w is expressed in terms of the 9 corner degrees of freedom:

$$w = \langle \phi_{(3)} \rangle \{r\} \tag{A.1}$$

where

$$\{r\} = \begin{Bmatrix} w_1 \\ \theta_{x1} \\ \theta_{y1} \\ w_2 \\ \theta_{x2} \\ \theta_{y2} \\ w_3 \\ \theta_{x3} \\ \theta_{y3} \end{Bmatrix}, \quad \langle \phi_{(3)} \rangle^T = \begin{Bmatrix} \zeta_1^2 (3-2\zeta_1) + 2\zeta_1\zeta_2\zeta_3 \\ \zeta_1^2 (b_3\zeta_2 - b_2\zeta_3) + (b_3 - b_2)\, \zeta_1\zeta_2\zeta_3/2 \\ \zeta_1^2 (a_3\zeta_2 - a_2\zeta_3) + (a_3 - a_2)\, \zeta_1\zeta_2\zeta_3/2 \\ \zeta_2^2 (3 - 2\,\zeta_2) + 2\,\zeta_1\zeta_2\zeta_3 \\ \zeta_2^2 (b_1\zeta_3 - b_3\zeta_1) + (b_1 - b_3)\, \zeta_1\zeta_2\zeta_3/2 \\ \zeta_2^2 (a_1\zeta_3 - a_3\zeta_1) + (a_1 - a_3)\, \zeta_1\zeta_2\zeta_3/2 \\ \zeta_3^2 (3 - 2\,\zeta_3) + 2\,\zeta_1\zeta_2\zeta_3 \\ \zeta_3^2 (b_2\zeta_1 - b_1\zeta_2) + (b_2 - b_1)\, \zeta_1\zeta_2\zeta_3/2 \\ \zeta_3^2 (a_2\zeta_1 - a_1\zeta_2) + (a_2 - a_1)\, \zeta_1\zeta_2\zeta_3/2 \end{Bmatrix} \tag{A.2}$$

and ζ_i are triangular coordinates as defined in Fig. A.2. By using these coordinates, the integration over the triangle can be carried out very simply. a_i and b_i are defined in Fig. A.1.

Differentiating $< \phi_{(3)} >$ with respect to x and y yields the interpolation functions $< \phi_x >$ and $< \phi_y >$ required to find the geometric stiffness matrix:

$$[k_G] = \int_A [\Phi_x^T \,\vdots\, \Phi_y^T] \begin{bmatrix} N_x & N_{xy} \\ N_{xy} & N_y \end{bmatrix} \begin{bmatrix} \Phi_x \\ \vdots \\ \Phi_y \end{bmatrix} dA \qquad (A.3)$$

Direct integration of (A.3) would, however, lead to extremely complicated expressions. An interpolation on the derivatives $w_{,x}$ and $w_{,y}$ which have a quadratic variation over the element, makes the derivation simpler. Six nodal point values, $\{\bar{w}_{,x}\}$, $\{\bar{w}_{,y}\}$, three at the corners and three at the midpoints of sides, are used.

$$w_{,x} = < \Phi_{(2)} > \{\bar{w}_{,x}\} \qquad (A.4)$$

$$w_{,y} = < \Phi_{(2)} > \{\bar{w}_{,y}\} \qquad (A.5)$$

$$\{\bar{w}_{,x}\} = [U]\{r\} \qquad (A.6)$$

$$\{\bar{w}_{,y}\} \quad [V]\{r\} \qquad (A.7)$$

where

$$< \Phi_{(2)} >^T = \begin{Bmatrix} \zeta_1 (2\zeta_1 - 1) \\ \zeta_2 (2\zeta_2 - 1) \\ \zeta_3 (2\zeta_3 - 1) \\ 4\zeta_1 \zeta_2 \\ 4\zeta_2 \zeta_3 \\ 4\zeta_3 \zeta_1 \end{Bmatrix} \qquad (A.8)$$

$a_i = (x_k - x_j)$

$b_i = (y_j - y_k)$

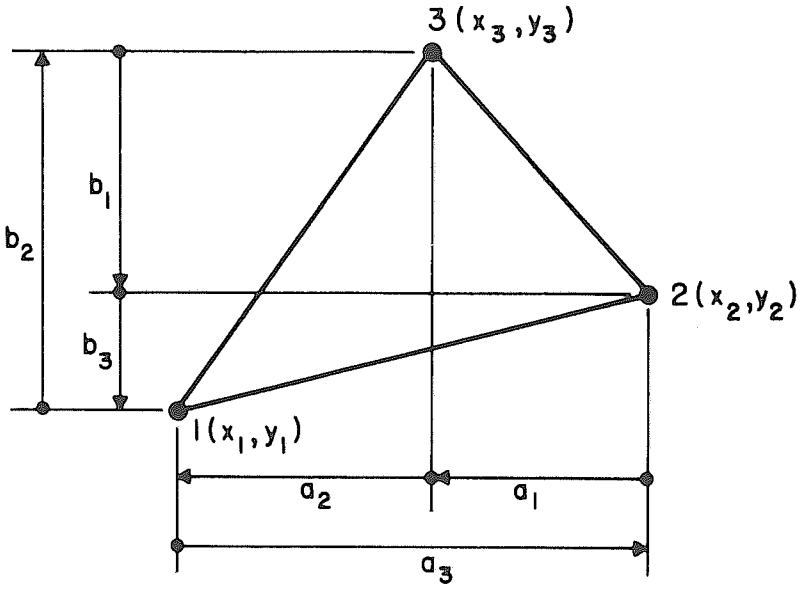

FIG. A.1 GEOMETRY OF TRIANGLE

$\zeta_i = A_i / A$

$\zeta_1 + \zeta_2 + \zeta_3 = 1$

$A_1 + A_2 + A_3 = A$

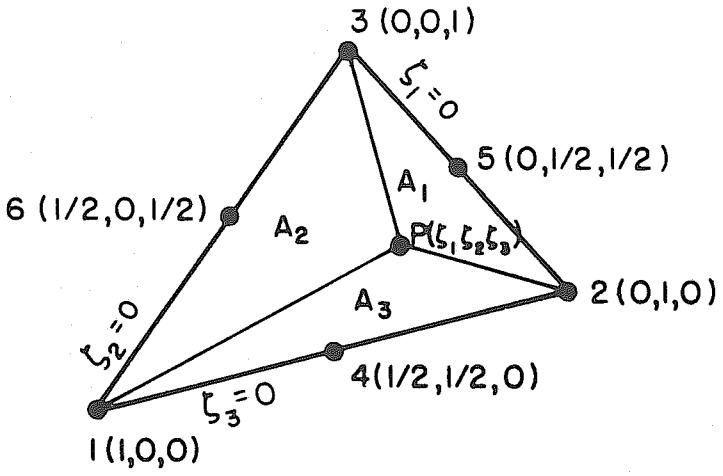

FIG. A.2 TRIANGULAR COORDINATES

$$U=\frac{1}{4A}$$

0	0	4A	0	0	0	0	0	0
0	0	0	0	0	4A	0	0	0
0	0	0	0	0	0	0	0	4A
$3b_1+b_3$	$b_1b_3+\frac{b_3}{4}(b_3-b_2)$	$b_1a_3+\frac{b_3}{4}(a_3-a_2)+A$	$3b_2+b_3$	$-b_2b_3+\frac{b_3}{4}(b_1-b_3)$	$-b_2a_3+\frac{b_3}{4}(a_1-a_3)+A$	b_3	$\frac{b_3}{4}(b_2-b_1)$	$\frac{b_3}{4}(a_2-a_1)$
b_1	$\frac{b_1}{4}(b_3-b_2)$	$\frac{b_1}{4}(a_3-a_2)$	$3b_2+b_1$	$b_2b_1+\frac{b_1}{4}(b_1-b_3)$	$b_2a_1+\frac{b_1}{4}(a_1-a_3)+A$	$3b_3+b_1$	$-b_3b_1+\frac{b_1}{4}(b_2-b_1)$	$-b_3a_1+\frac{b_1}{4}(a_2-a_1)+A$
$3b_1+b_2$	$-b_1b_2+\frac{b_2}{4}(b_3-b_2)$	$-b_1a_2+\frac{b_2}{4}(a_3-a_2)+A$	b_2	$\frac{b_2}{4}(b_1-b_3)$	$\frac{b_2}{4}(a_1-a_3)$	$3b_3+b_2$	$b_3b_2+\frac{b_2}{4}(b_2-b_1)$	$b_3a_2+\frac{b_2}{4}(a_2-a_1)+A$

(A.9)

$$V=\frac{1}{4A}$$

0	-4A	0	0	0	0	0	0	0
0	0	0	0	-4A	0	0	0	0
0	0	0	0	0	0	0	-4A	0
$3a_1+a_3$	$a_1b_3+\frac{a_3}{4}(b_3-b_2)-A$	$a_1a_3+\frac{a_3}{4}(a_3-a_2)$	$3a_2+a_3$	$-a_2b_3+\frac{a_3}{4}(b_1-b_3)-A$	$-a_2a_3+\frac{a_3}{4}(a_1-a_3)$	a_3	$\frac{a_3}{4}(b_2-b_1)$	$\frac{a_3}{4}(a_2-a_1)$
a_1	$\frac{a_1}{4}(b_3-b_2)$	$\frac{a_1}{4}(a_3-a_2)$	$3a_2+a_1$	$a_2b_1+\frac{a_1}{4}(b_1-b_3)-A$	$a_2a_1+\frac{a_1}{4}(a_1-a_3)$	$3a_3+a_1$	$-a_3b_1+\frac{a_1}{4}(b_2-b_1)-A$	$-a_3a_1+\frac{a_1}{4}(a_2-a_1)$
$3a_1+a_2$	$-a_1b_2+\frac{a_2}{4}(b_3-b_2)-A$	$-a_1a_2+\frac{a_2}{4}(a_3-a_2)$	a_2	$\frac{a_2}{4}(b_1-b_3)$	$\frac{a_2}{4}(a_1-a_3)$	$3a_3+a_2$	$a_3b_2+\frac{a_2}{4}(b_2-b_1)-A$	$a_3a_2+\frac{a_2}{4}(a_2-a_1)$

The rows in U and V are found by substituting nodal point values of ζ_1, ζ_2 and ζ_3 for each of the six nodal points into $< \Phi_x >$ and $< \Phi_y >$. The advantages of this extra step is that the matrices [U] and [V] can be kept outside the integration over the area.

Thus

$$[k_G] = [G]^T \int_A \begin{bmatrix} \Phi^T_{(2)} & 0 \\ 0 & \Phi^T_{(2)} \end{bmatrix} \begin{bmatrix} N_x & N_{xy} \\ N_{xy} & N_y \end{bmatrix} \begin{bmatrix} \Phi_{(2)} & 0 \\ 0 & \Phi_{(2)} \end{bmatrix} dA \; [G] \qquad (A.10)$$

(9x9) (9x12) (12x2) (2x2) (2x12) (12x9)

or

$$[k_G] = [G]^T [M] [G] \qquad (A.11)$$

where

$$[G] = \begin{bmatrix} U \\ V \end{bmatrix} \qquad (A.12)$$

$$[M] = \int_A \begin{bmatrix} \Phi^T_{(2)} & N_x & \Phi_{(2)} & \Phi^T_{(2)} & N_{xy} & \Phi_{(2)} \\ \Phi^T_{(2)} & N_{xy} & \Phi_{(2)} & \Phi^T_{(2)} & N_y & \Phi_{(2)} \end{bmatrix} dA = \begin{bmatrix} M_{11} & M_{12} \\ M_{21} & M_{22} \end{bmatrix} \qquad (A.13)$$

The inplane forces are assumed to have a linear variation over the triangle:

$$N_x = t < \zeta > \{\bar{\sigma}_x\} \qquad (A.14)$$

where

$$< \zeta >^T = \begin{Bmatrix} \zeta_1 \\ \zeta_2 \\ \zeta_3 \end{Bmatrix} \qquad \{\bar{\sigma}_x\} = \begin{Bmatrix} \sigma_{x_1} \\ \sigma_{x_2} \\ \sigma_{x_3} \end{Bmatrix} \qquad (A.15)$$

and t is the plate thickness.

σ_{xi} are the nodal point values of the σ_x stress. In the same way, N_y and N_{xy} are linear functions of σ_{yi} and τ_{xyi}, respectively.

Substituting (A.14) into (A.13) yields the following expression for the integrals:

$$[M_{11}] = \int_A \langle\Phi_{(2)}\rangle^T \langle\zeta\rangle \{\bar{\sigma}_x\} (\Phi_{(2)})\, dA = \sigma_{x1}[Q_1] + \sigma_{x2}[Q_2] + \sigma_{x3}[Q_3] \quad (A.16)$$

(6x6) (6x1) (1x3)(3x1)(1x6) (6x6) (6x6) (6x6)

$$[M_{12}] = \int_A \langle\Phi_{(2)}\rangle^T \langle\zeta\rangle \{\bar{\tau}_{xy}\} (\Phi_{(2)})\, dA = \tau_{xy_1}[Q_1] + \tau_{xy_2}[Q_2] + \tau_{xy_3}[Q_3] \quad (A.17)$$

$$[M_{21}] = [M_{12}]^T \quad (A.18)$$

$$M_{22} = \int_A \langle\Phi_{(2)}\rangle^T \langle\zeta\rangle \{\bar{\sigma}_y\} \langle\Phi_2\rangle\, dA = \sigma_{y_1}[Q_1] + \sigma_{y_2}[Q_2] + \sigma_{y_3}[Q_3] \quad (A.19)$$

where

$$[Q_1] = t \int_A \zeta_1 \langle\Phi_{(2)}\rangle^T \langle\Phi_{(2)}\rangle\, dA \quad (A.20)$$

$$[Q_2] = t \int_A \zeta_2 \langle\Phi_{(2)}\rangle^T \langle\Phi_{(2)}\rangle\, dA \quad (A.21)$$

$$[Q_3] = t \int_A \zeta_3 \langle\Phi_{(2)}\rangle^T \langle\Phi_{(2)}\rangle\, dA \quad (A.22)$$

Carring out the integration in A.20 yields:

$$[Q_1] = \frac{At}{1260}\left[\begin{array}{ccc:ccc} 30 & -4 & -4 & 12 & -4 & 12 \\ -4 & 6 & 1 & -8 & -4 & -12 \\ -4 & 1 & 6 & -12 & -4 & -8 \\ \hdashline 12 & -8 & -12 & 96 & 32 & 48 \\ -4 & -4 & -4 & 32 & 32 & 32 \\ 12 & -12 & -8 & 48 & 32 & 96 \end{array}\right]$$

The integration has been carried out by using the tables of area integrals presented by Felippa [14]. $[Q_2]$ and $[Q_3]$ are obtained from $[Q_1]$ by cyclic permutation of terms in the 3 x 3 submatrices of $[Q_1]$. The geometric stiffness metrix $[k_G]$ can now be computed if the inplane stress distribution defined by $\{\bar{\sigma}_x\}$, $\{\bar{\sigma}_y\}$ and $\{\bar{\sigma}_{xy}\}$, the corner point coordinates x_i, y_i, $i = 1, 3$, and plate thickness t are given.

It is quite interesting to note that the derivation of the geometric stiffness matrix using a cubic expansion for w, is almost exactly parallel to the derivation of the stiffness matrix for the quadratically varying strain triangular element (QST) with linearly varying thickness, which has been derived by Felippa [14].

Security Classification

DOCUMENT CONTROL DATA - R & D

(Security classification of title, body of abstract and indexing annotation must be entered when the overall report is classified)

1. ORIGINATING ACTIVITY *(Corporate author)* Department of Civil Engineering, Division of Structural Engineering and Structural Mechanics, University of California, Berkeley	2a. REPORT SECURITY CLASSIFICATION Unclassified 2b. GROUP ---

3. REPORT TITLE

A COMPUTER PROGRAM FOR ANALYSIS OF STIFFENED PLATES UNDER COMBINED INPLANE AND LATERAL LOADS

4. DESCRIPTIVE NOTES *(Type of report and inclusive dates)*

Technical Report

5. AUTHOR(S) *(First name, middle initial, last name)*

Dag Kavlie and Ray W. Clough

6. REPORT DATE March 1971	7a. TOTAL NO. OF PAGES 64	7b. NO. OF REFS 15
8a. CONTRACT OR GRANT NO. N 00014-67-A-0114-0020 b. PROJECT NO. SF 013 0301 c. d.	9a. ORIGINATOR'S REPORT NUMBER(S) UCSESM 71-4 9b. OTHER REPORT NO(S) *(Any other numbers that may be assigned this report)* ---	

10. Distribution Statement

THIS DOCUMENT HAS BEEN APPROVED FOR PUBLIC RELEASE AND SALE, ITS DISTRIBUTION IS UNLIMITED.

11. SUPPLEMENTARY NOTES ---	12. SPONSORING MILITARY ACTIVITY Naval Ship Research and Development Center, Department of the Navy Washington, D.C. 20007

13. ABSTRACT

The finite element method is used as the basis of a computer program for analysis of stiffened plates. Triangular and quadrilateral plate elements and beam elements may be used for idealization of the stiffened plates. The plate elements may have isotropic or orthotropic material properties. The stiffeners are assumed to be symmetric about the midplane of the plate. This assumption uncouples the plane stress and the plate bending problems. If the inplane stresses are not known in advance, the plane stress problem can be solved as a first step. The next step may be to solve the plate bending problem. The effect of the membrane stresses on the plate bending behavior is taken care of in this case by adding the geometric stiffness matrix to the elastic stiffness matrix. Alternatively the stability problem may be solved, finding the critical buckling eigenvalue and the corresponding mode shape. A listing of the FORTRAN IV computer program is given in the report, and a few examples of bending and buckling of stiffened plates are presented. The program has been developed and tested on the CDC 6400 computer.